

**RIGA TECHNICAL UNIVERSITY**  
Faculty of Power and Electrical Engineering  
Institute of Energy Systems and Environment

**Ruta Vanaga**

Doctoral Student of the Study Programme “Environmental Science”

**CLIMATE ADAPTIVE BUILDING SHELL FOR NEARLY  
ZERO ENERGY BUILDINGS: APPLICATION OF  
BIOMIMICRY PRINCIPLES**

**Summary of the Doctoral Thesis**

Scientific Supervisors  
Professor Dr. sc. ing.  
ANDRA BLUMBERGA

Professor Dr. habil. sc. ing.  
DAGNIJA BLUMBERGA

RTU Press  
Riga 2019

Vanaga, R. Climate Adaptive Building Shell for Nearly Zero Energy Buildings: Application of Biomimicry Principles. Summary of the Doctoral Thesis. Riga: RTU Press, 2019. 47 p.

Published in accordance with the decision of the Faculty of Power and Electrical Engineering, Institute of Energy Systems and Environment of 1 November 2018, Minutes No. 100.

The work has been supported by the National Research Program “Energy efficient and low-carbon solutions for a secure, sustainable and climate variability reducing energy supply (LATENERGI)”.

**ISBN**      **978-9934-22-245-0 (print)**  
                 **978-9934-22-248-1 (pdf)**

# **DOCTORAL THESIS PROPOSED TO RIGA TECHNICAL UNIVERSITY FOR THE PROMOTION TO THE SCIENTIFIC DEGREE OF DOCTOR OF ENVIRONMENTAL ENGINEERING**

To be granted the scientific degree of Doctor of Environmental Engineering, the present Doctoral Thesis has been submitted for the defence at the open meeting of RTU Promotion Council on 11 April 2019 at the Faculty of Power and Electrical Engineering of Riga Technical University, 12/1 Āzenes Street, Room 115.

## **OFFICIAL REVIEWERS**

Dr. sc. ing. Gatis Bažbauers  
Riga Technical University

Dr. sc. ing. Ainis Lagzdīņš  
Latvia University of Life Sciences and Technologies, Latvia

Dr. Uli Jakob  
Stuttgart University of Applied Sciences, Germany

## **DECLARATION OF ACADEMIC INTEGRITY**

I hereby declare that the Doctoral Thesis submitted for the review to Riga Technical University for the promotion to the scientific degree of Doctor of Environmental Engineering is my own. I confirm that this Doctoral Thesis has not been submitted to any other university for the promotion to a scientific degree.

Ruta Vanaga ..... (signature)

Date .....

The Doctoral Thesis has been written in Latvian, it consists of an introduction; 5 chapters; conclusions; 122 figures; 33 tables; the total number of pages is 164. The Bibliography contains 220 titles.

# CONTENT

Abbreviations .....	4
Introduction .....	6
Objectives.....	7
Research methods.....	7
Scientific significance .....	8
Practical significance.....	8
Aprobation.....	9
Thesis outline .....	11
1. Biomimicry approach creating climate adaptive building shell element – building integrated solar energy storage Bi-SES .....	12
1.1. Defining the problem.....	12
1.2. Biologizing the question.....	12
1.3. Criteria for abstracting the best nature strategy .....	12
1.4. Natural environment vs built structures.....	13
1.5. Muti-criteria decision making methodology for biomimicry. Choosing the best nature strategy for Bi-SES.....	13
1.6. Innovative climate adaptive solar energy storage element Bi-SES, emulating nature strategies	16
1.7. Concept of innovative climate adaptive solar energy storage element Bi-SES.....	18
2. Experimental research of climate adaptive building shell element Bi-SES.....	22
2.1. Experiment I. Choosing the phase change material: paraffin, slat hydrates, fatty acids .....	22
2.2. Experiment II. Comparison of Bi-SES with the reference wall .....	30
3. Mathematical modelling of Climate adaptive module Bi-SES-II.....	34
3.1. Mathematical modelling in <i>COMSOL Multiphysics</i> , heat transfer processes, boundary conditions .....	34
3.2. Numerical study.....	35
3.3. Simulation output .....	36
3.4. Validation of simulation model .....	36
3.5. Simulation results analysis .....	37
4. Climate adaptive facade module Bi-SES incorporated in building.....	41
Conclusions .....	44
References .....	44

## ABBREVIATIONS

<p>EU – European Union          LV – Republic of Latvia          MK – Cabinet of Ministers          netZEB – Net zero energy building          nZEB – Nearly zero energy building          IEA – International Energy Agency          A/V ratio – Building thermal envelope ratio to heated volume          CABS – Climate adaptive building shell          Bi-SES – Building Integrated Solar Energy Storage          DSC – Differential scanning calorimetry          DF – Double facade</p>	<p>EPBD – Energy Performance of Buildings Directive.          GHG – Greenhouse Gasses          EFTE – Ethylene tetrafluoroethylene          PV – Photovoltaics          LED – light-emitting diode          XPS – Extruded polystyrene insulation          LA – lauric acid          SA – stearic acid          MA – myristic acid          PA – palmitic acid          CA – capric acid          PCM – phase change material          LMoCA – Latvian Museum of Contemporary Art          AHP – Analytical Hierarchy Process          ASHRAE – American Society of Heating, Refrigerating and Air-Conditioning Engineers</p>
--	---

<p><math>n_{50}</math> – Air Change Rate at 50 Pa  <math>\lambda</math> – conductivity, W/(m K)  <math>U</math> – heat transfer coefficient, W/(m<sup>2</sup>K)  <math>\rho</math> – density kg/m<sup>3</sup>  <math>C_{ap}</math> – average specific heat between <math>T_i</math> and <math>T_f</math>, J/(kg K)  <math>C_{1p}</math> – vidējais īpatnējā siltumietilpība starp <math>T_m</math> un <math>T_i</math>, J/(kg K)  <math>C_{sp}</math> – average specific heat between <math>T_i</math> un <math>T_m</math>, J/(kg K)  <math>H_i</math> – molar melting heat of component <math>i</math> at the melting point T, J/mol  <math>Q</math> – amount of stored heat, kJ  <math>Q_l</math> – absorbed latent heat, J  <math>Q_s</math> – absorbed sensible heat, J  <math>R</math> – gas constant 8,314 J/(mol K)  <math>T_s</math> – surface temperature, °C  <math>T_{sur}</math> – surrounding temperature, °C</p>	<p><math>T_e</math> – temperature of eutectic point, K  <math>T_f</math> – final temperature, °C  <math>T_i</math> – initial temperature, °C  <math>T_{ie}</math> – the melting point of component I, K  <math>T_m</math> – melting temperature, °C  <math>a_m</math> – melted fraction  <math>c_i</math> – specific heat of each of the <math>i</math> components, kJ/kg  <math>c_p</math> – specific heat, kJ/kg  <math>c_{pm}</math> – modified specific heat, kJ/kg  <math>h</math> – latent heat of fusion, kJ/kg;  <math>i</math> – generally valued as 1 or 2  <math>m</math> – mass of material, kg;  <math>m_e</math> – mass of eutectic mixture, g;  <math>m_{fi}</math> – mass of fatty acid, g;  <math>wt\%_{fi}</math> – mass ratio of one fatty acid in %  <math>x_i</math> – composition of eutectic mixture (mole percent)  <math>\Delta h_m</math> – heat of fusion per unit mass (J/kg)  <math>\Delta T_m</math> – melting temperature range, K  <math>\Delta H</math> – enthalpy difference, kJ/kg;</p>
--	--

## INTRODUCTION

The current EU climate and energy framework sets three key targets by 2020: 1) to ensure a 20 % reduction in GHG emissions compared to 1990 levels; 2) to ensure the use of 20 % renewable energy in energy production; 3) to improve energy efficiency by 20 %. Considering that the building sector is one of the largest energy consumers and GHG producers (material production, construction, building heating, cooling), improving the energy efficiency of buildings can bring us closer to the set goals.

Since building sector accounts for 40 % of energy consumption in EU, it is the target for energy efficiency measures. Directive 2010/31/EU of the European Parliament and of the Council of 19 May 2010 on the energy performance of buildings provides a framework for Member States to reduce energy consumption and increase the use of renewable energy (preferably produced locally or nearby) in the building sector. All Member States should ensure that by 31 December 2020 all new buildings are nearly zero-energy buildings (nZEB). The minimum energy performance requirements for nZEB shall be determined by each Member State based on positive investment and running costs balance during the estimated lifetime of the building. The nZEB level set in Latvian legislation is  $< 45 \text{ kWh}/(\text{m}^2\text{g})$  for energy demand for heating. In buildings where the principles of low-energy building design (successful architectural composition, A/V ratio, the use of solar thermal benefits, the ratio of glazed and opaque surfaces) can be applied investments for achieving nZEB benchmark will be feasible. Conversely, in buildings facing functional or technical constraints in applying the principles, it may not be economically feasible to achieve an nZEB level with traditional energy efficiency improvement techniques.

Currently, thermal insulation products with improved thermal properties are available on the market (polyurethane, polyisocyanurate  $\sim 0.023 \text{ W}/(\text{m K})$ ). In the near future “super insulating materials” with conductivity two times better (aerogel  $\sim 0.013 \text{ W}/(\text{m K})$ ), or even 10 times better (vacuum panels  $\sim 0.0035 \text{ W}/(\text{m K})$ ) will be introduced to common practice. Effective air handling units play a major role in improving energy efficiency. The efficiency of ventilation systems is now greatly improved and can recover up to 93 % of heat. However, further improvement of traditional energy efficiency measures is approaching its limits (improved thermal conductivity for thermal insulation materials, thermal properties of windows, efficiency of ventilation systems), therefore it is necessary to introduce conceptually new ideas for energy efficiency of buildings. The International Energy Agency (IEA) points out the need for energy-flexible buildings – the ability to manage energy needs and production according to local climatic conditions, user needs and network requirements. One of the options is the *on-site* energy production and accumulation in the building envelope.

There is an urge in paradigm shift – a transition from building envelope structures with static, regressing in time properties to dynamic, demand responsive building envelope properties is required. Climate adaptive building shell (CABS) offers a solution – building envelope with dynamic thermal properties. CABS can repeatedly and reversibly change some of its functions by responding to changing thermal requirements and different boundary conditions, with the aim of improving the overall building energy performance.

Conceptually new ideas for CABS can be developed using a biomimicry approach. It encourages looking for inspiration in nature, where “solutions” have been developed over 3.8 billion years. According to the biomimicry methodology, there are two approaches to develop new designs: 1) *challenge to biology* – where the problem that needs a solution is initially defined and then the solutions are sought in nature; or 2) *biology to the challenge* – where the idea found in nature serves as an inspiration for technical design. The Doctoral Thesis is mainly based on the first approach. The defined problem is “to develop innovative climate adaptive building thermal envelope that actively contributes providing constant microclimate (temperature) ensuring solar energy storage”.

Looking for inspiration in nature thermoregulation strategies in living beings were studied, focusing more on the animals of the northern climate. The building envelope, like animal skin, is like an interlayer between the internal environment, where constant temperature is to be ensured, and the external environment exposed to changing external conditions. Therefore, inspiration was sought in animal thermoregulation strategies, paying attention to the processes taking place in the skin of the animals.

## OBJECTIVES

The aim of the Doctoral Thesis is to develop a conceptually new design for climate adaptive building shell using innovative research methods. The main task of the designed element is to collect, store and release solar energy efficiently. The proposed solution must be able to respond to changes in environmental climatic conditions. It should increase the energy flexibility of the building by supporting the priorities set by the IEA.

To achieve the goal, the following tasks were set.

1. To follow the biomimicry methodology in developing the design.
2. To summarize living being’s thermoregulation strategies maintaining constant core temperature.
3. To identify the most suitable thermoregulation strategy to mimic in climate adaptive building shell – solar energy storage wall.
4. To develop a concept for climate adaptive building shell – solar energy storage wall.
5. To perform mathematical modelling and simulation for developed CABS concept using *COMSOL Multiphysics 5.1*.
6. To make a prototype of the developed CABS proposal and to perform an experiment in real climatic conditions.
7. To validate the calculation model with the data obtained in the experiment.
8. To describe the example of the way to incorporate the developed CABS in building design.

## RESEARCH METHODS

Both qualitative and quantitative scientific research methods have been used in the Doctoral Thesis: literature review, case study, data collection and analysis, as well as laboratory experiments and experiments in real climatic circumstances and mathematical modelling for testing the hypothesis.

At the beginning of the research, the analysis of scientific literature was carried out by summarizing the normative acts of energy efficiency of buildings of Latvia and the EU and the goals set and by reviewing the latest innovations in building thermal envelope sector.

In order to create innovative CABS with the biomimicry method, the study explores various thermoregulation strategies in nature and, using a multi-criteria analysis, identifies a strategy with the greatest potential for imitating in a conceptually new building envelope design.

Chapter 2 deals with developed concept of climate adaptive building shell – solar energy storage wall based on imitation of thermoregulation strategies found in nature. Chapter 3 describes prototype design and experiment. Two experiments were carried out within the framework of the research: 1) comparison of different phase change materials; 2) laboratory testing of the facade module. Chapter 4 discusses the mathematical modelling of the developed concept in *COMSOL* software and its verification against the experimental data. Chapter 5 presents the application of the developed solution in the building.

## **SCIENTIFIC SIGNIFICANCE**

The theme of the Doctoral Thesis is scientifically significant both in Latvia and internationally, since there is an urge for conceptually new ideas for decarbonizing buildings, considering global warming risks and European Union guidelines for increasing energy efficiency of buildings.

- For the first time in Latvia, the solution of building envelope construction based on biomimicry approach was developed.
- A methodology for the use of multi-criteria analysis in the biomimicry approach has been developed.
- A prototype of innovative climate adaptive facade module has been developed.
- Use of different phase transition materials and heat conductivity accelerators for climate adaptive facade module is approved;
- A methodology for integrating climate adaptive facade module in the building has been developed.

Work can serve as an example in several aspects. Firstly, it is the use of biomimicry techniques to develop new solutions; secondly, the use of multicriteria analysis for biomimicry approach by evaluating different possible directions of development and by determining the direction with the greatest potential; thirdly, choosing the most suitable phase change material for use in the building thermal envelope; and, fourthly, developed climate adaptive building shell element can serve as a basis for further energy efficient building envelope designs.

## **PRACTICAL SIGNIFICANCE**

The Doctoral Thesis has a high practical value. The developed climate adaptive building shell element can be used everywhere in the temperate climate zone. The obtained results provide new information on the behaviour of different phase change materials in real climatic

conditions, on the use of different metals to accelerate the phase change, on the behaviour of the complex, multi-component climate adaptive facade module under real climatic conditions.

The results of the Doctoral Thesis can be further used to promote both the use of biomimicry methods and development of new concepts for building envelope with dynamic properties ensuring positive energy contribution to the overall energy balance of the building. The research carried out may also be useful in developing new methods for calculating the energy performance of buildings, including the ability of the building envelope to accumulate energy.

## APROBATION

Research results have been published in the following journals.

1. Vanaga, R., Blumberga, A., Freimanis, R., Mols, T., Blumberga, D. Solar Facade Module for Nearly Zero Energy Building. *Energy*, 2018, Vol. 157, pp. 1025–1034. ISSN 0360-5442. Available from: doi:10.1016/j.energy.2018.04.167.
2. Biseniece, E., Žogla, G., Kamenders, A., Purviņš, R., Kašs, K., Vanaga, R., Blumberga, A. Thermal Performance of Internally Insulated Historic Brick Building in Cold Climate: A Long Term Case Study. *Energy and Buildings*, 2017, Vol. 152, pp. 577–586. ISSN 0378-7788. Available from: doi:10.1016/j.enbuild.2017.07.082.
3. Vanaga, R., Blumberga, A., Gušča, J., Blumberga, D. Choosing the best nature's strategy with the highest thermodynamical potential for applicatin in building thermal envelope using MCA analysis. In: *Energy Procedia*, Shanghai, China, 5-7 June, 2018. Germany: Elsevier, 2018, pp. 450–455. Available from: doi:10.1016/j.egypro.2018.09.252.
4. Mols, T., Dzene, K., Vanaga, R., Freimanis, R., Blumberga, A. Experimental Study of Small-Scale Passive Solar Wall Module with Phase Change Material and Fresnel Lens. In: *Energy Procedia*, Latvia, Riga, 16–18 May 2018. Germany: Elsevier, 2018, pp. 467–473. ISSN 1876-6102. Available from: doi:10.1016/j.egypro.2018.07.048.
5. Vanaga, R., Purviņš, R., Blumberga, A., Veidenbergs, I., Blumberga, D. Heat Transfer Analysis by Use Of Lense Integrated in Building Wall. In: *Energy Procedia*, Latvia, Rīga, 10–12 May, 2017. Germany: Elsevier, 2017, pp. 453–460. ISSN 1876-6102. Available from: doi:10.1016/j.egypro.2017.09.030.
6. Zamovskis, M., Vanaga, R., Blumberga, A. Mathematical Modelling of Performance of New Type of Climate Adaptive Building Shell. In: *Energy Procedia*, Latvia, Riga, 12–14 October 2016. Germany: Elsevier, 2017, pp. 270–276. ISSN 1876-6102. Available from: doi:10.1016/j.egypro.2017.04.065.
7. Kancane, L., Vanaga, R., Blumberga, A. Modeling of Building Envelope's Thermal Properties by Applying Phase Change Materials. *Energy Procedia*, 2016, Vol. 95, pp. 175–180. ISSN 1876-6102. Available from: doi:10.1016/j.egypro.2016.09.041.
8. Kamenders, A., Rušenieks, R., Vanaga, R., Rochas, C., Blumberga, A. Nearly Zero Energy Building (nZEB) in Latvia. In: *9th International Conference on Environmental Engineering (ICEE): Selected Papers*, Lithuania, Vilnius, 22–24 May 2014. Vilnius: Vilnius Gediminas Technical University Press Technika, 2014, pp. 1–8. e-ISBN 978-609-457-640-9. e-ISSN 2029-7092. Available from: doi:10.3846/enviro.2014.263.
9. Vanaga, R., Blumberga, A. First Steps to Develop Biomimicry Ideas. *Energy Procedia*, 2015, Vol. 72, pp. 307–309. ISSN 1876-6102. Available from: doi:10.1016/j.egypro.2015.06.044.

Research results have been discussed at the following conferences.

1. Blumberga, A., Biseniece, E., Purviņš, R., Kamenders, A., Žogla, G., Blumberga, D., Vanaga, R. Vēsturisko ēku energoefektivitātes paaugstināšana aukstajā klimatiskajā zonā. Caturtais pasaulei atgališu saīss. Latgolys simtgadis kongress, 5 May 2017, Rēzekne, Latvia.
2. Vanaga, R., Blumberga, A., Gušča, J., Blumberga, D. Choosing the best nature's strategy with the highest thermodynamical potential for application in building thermal envelope using MCA analysis. CUE2018-Applied Energy Symposium and Forum 2018: Low carbon cities and urban energy systems, 6 June 2018, Shanghai, China.
3. Mols, T., Dzene, K., Vanaga, R., Freimanis, R., Blumberga, A. Experimental Study of Small-Scale Passive Solar Wall Module with Phase Change Material and Fresnel Lens. International Scientific Conference on Environmental and Climate Technologies, CONECT 2018, 16 May 2018, Riga, Latvia.
4. Vanaga, R., Purviņš, R., Blumberga, A., Veidenbergs, I., Blumberga, D. Heat Transfer Analysis by Use of Lense Integrated in Building Wall. International Scientific Conference on Environmental and Climate Technologies, CONECT 2017, 10 May 2017, Riga, Latvia.
5. Zamovskis, M., Vanaga, R., Blumberga, A. Mathematical Modelling of Performance of New Type of Climate Adaptive Building Shell. International Scientific Conference on Environmental and Climate Technologies, CONECT 2016, 12 October 2016, Riga, Latvia.
6. Kancane, L., Vanaga, R., Blumberga, A. Modeling of Building Envelope's Thermal Properties by Applying Phase Change Materials. International Scientific Conference on Environmental and Climate Technologies, CONECT 2015, 14 October 2015, Rīga, Latvija.
7. Kamenders, A., Rušenieks, R., Vanaga, R., Rochas, C., Blumberga, A. Nearly Zero Energy Building (nZEB) in Latvia. 9th International Conference on Environmental Engineering (ICEE): Selected Papers, 22 May 2014, Vilnius, Lithuania.
8. Kamenders, A., Vanaga, R., Biseniece, E., Blumberga, A. Cost-Optimal Energy Performance Level for Apartment Buildings in Latvia. 27th International Conference on Efficiency, Cost, Optimization, Simulation and Environmental Impact of Energy Systems (ECOS 2014), 15 June 2014, Turku, Finland.
9. Vanaga, R., Blumberga, A. First Steps to Develop Biomimicry Ideas. In: *Abstracts of 55th International Scientific Conference: Subsection: Environmental and Climate Technologies*, Riga: RTU Press, 14–15 October, Riga, Latvia.
10. Vanaga, R., Kamenders, A., Krauklis, E. Reaching EnerPHit Standard Using Holistic Approach. 17th International Passive House Conference 2013, 19–20 April 2013, Frankfurt, Germany.
11. Kamenders, A., Vanaga, R., Krauklis, E. Post-Occupancy Evaluation of Dormitory Building with Aim of EnerPHit Renovation. 17th International Passive House Conference 2013, 19–20 April 2013, Frankfurt, Germany.

Other publications.

1. Kalniņš, S., Gušča, J., Valtere, S., Vanaga, R., Blumberga, D. Transition to Low Carbon Society. Evaluation Methodology. *Agronomy Research*, 2014, Vol. 12, No. 3, pp. 851–862. ISSN 1406-894X.
2. Timma, L., Vilgerts, J., Vanaga, R., Kļavenieks, K., Blumberga, D. Decomposition Analysis Based on IPAT and Kaya Identity for Assessment of Hazardous Waste Flow within Enterprise. In: *27th International Conference on Efficiency, Cost, Optimization, Simulation and Environmental Impact of Energy Systems: Conference Proceedings*, Finland, Turku, 15–19 June 2014. Turku: 2014, pp. 1–7.

3. Vanaga, R., Kamenders, A., Krauklis, E. Reaching EnerPHit Standard Using Holistic Approach. In: 17th International Passive House Conference 2013, Germany, Frankfurt, 19–20 April 2013. Frankfurt: Passive House Institute, 2013, pp. 149–150. ISBN 9783000413469.
4. Kamenders, A., Vanaga, R., Krauklis, E. Post-Occupancy Evaluation of Dormitory Building with Aim of EnerPHit Renovation. In: *17th International Passive House Conference 2013*, Germany, Frankfurt, 19–20 April 2013. Frankfurt: Passive House institute, 2013, pp. 533–538. ISBN 9783000413469.

## **THESIS OUTLINE**

The Doctoral Thesis is written in Latvian. It contains an introduction, five chapters, conclusions, and a list of references. The introduction of the Doctoral Thesis justifies the topicality of the topic, sets out the aim of the Thesis and the tasks to be performed, as well as describes the scientific and practical significance of the research. The first chapter of the Doctoral Thesis analyses the current situation in the field of energy efficiency of buildings, moving towards the introduction of nearly zero-energy buildings and examines the latest concepts for improving the thermal performance of building thermal envelope. The second chapter of the Thesis describes the concept of developed innovative climate adaptive building shell element based on the biomimicry method. The third chapter describes the prototype preparation and experiments; the fourth chapter describes the mathematical modelling of the prototype and the comparison with the experimental data. The fifth chapter describes the possible use of the developed prototype in a real building. At the end, conclusions are summarized. For a literature review, see the full version of the Doctoral Thesis.

# 1. BIOMIMICRY APPROACH CREATING CLIMATE ADAPTIVE BUILDING SHELL ELEMENT – BUILDING INTEGRATED SOLAR ENERGY STORAGE BI-SES

Biomimicry proposes two opposite approaches called Biomimicry Design Spirals [1]: 1) *challenge to biology* defines technological design problem and seeks for answer in nature; 2) *biology to design* explores particular strategy in nature and seeks for appropriate application.

In order to create a conceptually new biomimicry-based CABS proposal Bi-SES (*Building Integrated Solar Energy Storage*), following the biomimicry design spiral “challenge to biology”, the following tasks will be performed in the course of further development:

- 1) defining the problem;
- 2) biologizing the question;
- 3) setting selection criteria;
- 4) finding suitable strategies in nature;
- 5) identifying the strategy with the greatest potential with multi-criteria analysis;
- 6) imitating the nature strategy in the structure of the enclosing structure.

## 1.1. Defining the problem

The following problem is defined to be studied in this research – to create a building envelope able to contribute to the building’s energy balance by storing solar energy.

## 1.2. Biologizing the question

In line with the biomimicry methodology, the question must be biologized before looking for suitable strategies in the nature. The terminology of building construction technology needs to be adapted to biology [2].

Table 1.1

Technical Requirements for Solar Thermal Energy Storage Facade

Function	Technical requirements	Biologized questions
Minimal heat losses	High thermal resistance	Envelopes with high thermal resistance
	Adaptive thermal resistance	Envelopes with adaptive thermal resistance
Maximal heat gains	Solar energy transmittance	Solar energy transmittance
	Solar tracking	Solar tracking
	Heat gains in diffuse solar radiation	Best positions for solar gains, remaining in the shine
	Heat generation	Diffuse radiation caption Adaptation to changing conditions Heat generation processes in living organisms
Energy exchange	Energy capture	Energy production in living organisms, seasonal changes
	Energy storage	Energy storage substance in living organisms
	Energy release	Heat exchange processes with the surroundings

## 1.3. Criteria for abstracting the best nature strategy

In order to search for the most appropriate strategies in nature, the focus will be on living organisms’ thermoregulation processes, mainly in living organisms in the northern climate. The following selection criteria have been set.

Criteria for Abstracting the Best Nature Strategy

Function	Criterion
Energy production	Metabolic processes Thermoregulation
Energy storage	Seasonal changes in metabolic and thermoregulation processes
Energy exchange process adaptation to changing surrounding conditions	Thermoregulation optimisation strategies Adaptation mechanisms

#### 1.4. Natural environment vs built structures

Nature can serve as an inspiration for building energy efficiency. There are parallels in built and natural environments. Building thermal envelope serves as the border between the inner conditions and the surrounding environment. Building services cover heating, cooling or fresh air demand to maintain constant defined comfort settings. It is similar to endothermic animals whose metabolic heat ensures almost constant body temperature under large environmental temperature fluctuations. There is a wide range of thermoregulation strategies in living organisms – minimising/maximising metabolism, torpor, heat-exchangers, bypasses, etc. But vegetation has another important capability – to absorb CO<sub>2</sub> and release O<sub>2</sub> – important for reducing air exchange and related heat losses due to the exhaled CO<sub>2</sub>. These strategies can serve as an inspiration to maintain constant indoor environment. The indoor microclimate has three main components – temperature, humidity and air exchange. Within this work, only indoor temperature is considered (+22 °C) [3]–[12].

To maintain a constant temperature in the building, energy is needed for both heating and cooling. A heat source is internal, analogically to endothermic animals. The heat supply system is as a metabolic system where the “nutrition” produces necessary heat. For a thermo-neutral zone with a constant metabolic level, we will assume the time of the year when the building does not require heating or cooling (“metabolic rate” is constant and is zero). The lowest outdoor air temperature at which “metabolic rate” (heat production) must be increased is +8 °C for 5 days in a row. The summers of Latvia climate summer can be “survived” in buildings without defined indoor temperature by maintaining “metabolic rate” at thermo-neutral zone. In winter it is not possible to survive without increasing “metabolic rate”. Summer diurnal outdoor temperature is closer to the indoor temperature than winter. Therefore, when choosing the most appropriate nature strategy, the emphasis is on overcoming cold.

Various thermoregulation strategies have been studied. The most suitable for imitation in the building envelope were considered blubber, blood circulatory system, skin and plant hibernation strategy. Multi-criteria analysis was performed to select the most appropriate one.

#### 1.5. Multi-criteria decision making methodology for biomimicry. Choosing the best nature strategy for Bi-SES

Biomimicry design spiral is a complex hierarchy of criteria and alternatives and at some point there is a need to choose among the options – a typical *Multi Criteria Decision Making (MCDM)* problem [13], [14].

In “*challenge to biology*”, after defining a problem follow steps of biologizing the questions (setting the criteria) and discovering nature models (alternatives). Before abstracting the essence of nature strategies decision must be made – which alternative has more potential with respect to all criteria to achieve the overall goal. In this phase *MCDM* methods can help in decision making process. *AHP* method is recognized as the most appropriate method in this paper since the objective is not to eliminate any of alternatives but to obtain ranking of alternatives and to explore the impact of different aspects of alternatives in complex structure.

As stated in previous sections the goal of the study is to find the best alternative of nature strategies to apply for innovative thermal envelope with climate adaptive properties. For innovative building component design 7 important criteria are defined (see Table 1.3.).

Table 1.3

Criteria for Innovative Thermal Envelope With Climate Adaptive Properties

Criteria	Definition
1 <b>Transmission heat losses</b>	The first component in building energy demand balance is the transmission heat losses through the building thermal envelope. There is urgent need of improvement of building envelope transmission losses since traditional materials have exhausted further possibilities of improvement. Heat losses have to be minimised.
2 <b>Ventilation heat losses</b>	The second component in building energy demand balance is heat losses due to the infiltration and ventilation. The necessary air volume is related to fresh air requirements to replace polluted air (exhale (CO <sub>2</sub> ), volatile substances, and sources of pollution). Infiltration is due to leakages in building envelope. Each building construction can be characterised by air permeability indicator.
3 <b>Solar heat gains</b>	The third component in building energy demand balance is the solar heat gains. Nature is driven by solar energy. Solar heat gains play important role in low energy building design. Innovative envelope should explore the possibilities solar energy offers. There are more heat gains than losses through south oriented windows in winter season in Northern Hemisphere. Innovative building envelope has to explore the benefits of solar energy.
4 <b>Thermal inertia</b>	Thermal inertia has secondary impact on building energy demand, but it plays a more important role for low energy buildings. The building thermal inertia determines the amount useful heat gains that can reduce the energy consumption of the building for heating or cooling. Buildings with high thermal inertia are more resistant to outside temperature fluctuations both – in winter and in summer (in temperate climates with large temperature fluctuations).
5 <b>Energy storage</b>	Energy storage in building envelope is a new concept for building energy demand. It is one of the strategies how to become energy neutral over the year. Surplus energy in summer can be stored for winter.
6 <b>Energy production</b>	Building envelope integrated energy production is another rather new concept for building energy demand. Currently there are many examples of BIPV (Building Integrated Photovoltaic).
7 <b>Changing surface parameters</b>	Changing surface characteristics would help diminish heating and cooling energy demand due to the emissivity of the material. For example, for cooling season light coloured, reflective surfaces are favourable, but for heating season dark, absorbing facade is more preferable.

Nature is complex and versatile. Surviving strategies are locally adjusted and sustainable [15]. In the presented study 4 general strategies are chosen as alternatives to evaluate which of them has greater potential to serve as an example for innovative climate adaptive building shell (Table 1.4). *MCDM* methods do not give the best possible alternative of infinite options. They reflect the subjective choices of expert’s preferences [15], [16].

Table 1.4

Alternatives – Nature Strategies for Innovative Thermal Envelope With Climate Adaptive Properties

Alternative	Definition
1	<b>Blubber</b> Blubber is a subcutaneous fat layer found in cetaceans and serves both as a thermal insulator and energy storage substance. Metabolic energy is stored in blubber. The thickness and content of blubber varies seasonally and is based on location in the animal body.
2	<b>Blood circulation system</b> Blood circulation system is an important component in thermoregulation – it provides convective heat exchange in organisms. Convection is much more effective heat exchange process than conduction. Blood circulation system prevents or maximises heat loss, and its ability to adapt is very flexible, via circulation loops, bypasses and speed of circulation it can adapt both seasonally, daily, hourly.
3	<b>Skin</b> Animals in different climates have different skin properties – absorbing solar radiation (polar bear) or as a cooling substance (oversized elephant skin). Some animals can change the colour of their skin – from black when solar heat absorption is needed, to reflective coating when cooling is needed, or changing the size of chromatofores containing pigment. This alternative covers furs and coats, since those are closely related to the processes in skin (piloerection).
4	<b>Vegetation living and growing strategies</b> Nevertheless animal thermoregulation strategies are more obviously related to thermal processes in buildings. Vegetation surviving winter strategies could serve as an inspiration as well. Vegetation hibernate by adjusting cell solutes, anti-freeze in extracellular spaces, strengthening the cell membranes, waxing the surface of evergreen spruce. Vegetation life cycle strategies could be useful for building energy efficiency since energy production and CO <sub>2</sub> capture / O <sub>2</sub> release processes take place in vegetation cells.

In biomimicry the biologization phase is followed by the phase of discovering and extracting the essence of nature strategies. In case of different alternatives, the best one must be chosen to proceed to next phases of extracting and emulating. The defined goal, criteria (biologized questions) and alternatives (nature strategies) are the components of complex decision-making hierarchy.

### 1.5.1. Results and discussion

The priorities of the *AHP* show that the most important criterion for the development of innovative climate adaptive building shell, reflecting the author's choice, is energy storage. The next most important criterion is thermal inertia and other criteria are much less important. The overall priorities for each alternative are obtained by multiplying the weight of the respective criterion and summing the weighted local priorities.

Overall priority of alternatives gained in *AHP MCA* (Fig. 1.1) shows that blubber is the most promising thermoregulation strategy for innovative climate adaptive envelope technological design according to the author's knowledge on selected alternatives and obtained criteria weights. Blood circulation system comes as second and animal skin and vegetation has fewer capabilities according to the criterion weight. Although in the individual criteria ("Energy Production", "Solar Heat Benefits") plants and animal skin have the highest rating, these criteria are given a lower weight in the given job assignment, therefore, the common priorities of plant and animal skin are assessed lower. Changing the weight of the criteria would change the overall priorities. In this study, more weight was assigned to the criteria that might add new, dynamic features to the building envelope.

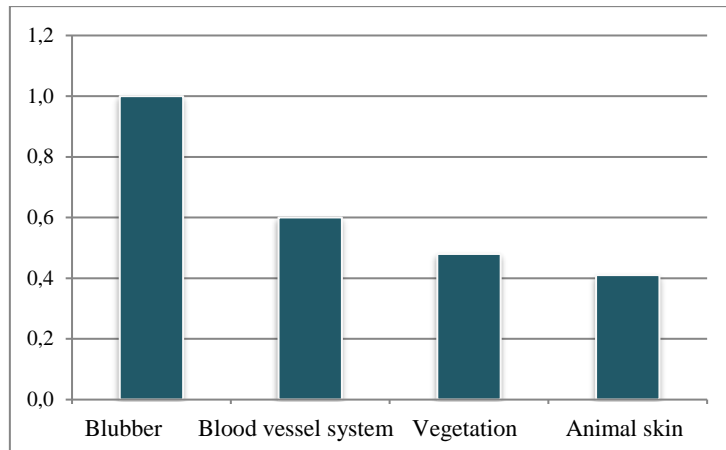


Fig. 1.1. Overall priorities for choosing the best nature strategy.

Fig. 1.1 reflects the dominance of the blubber over other natural strategies. At closer look (see full version), this dominance is obtained with the highest local priority in the “heaviest” criterion – “Energy Storage”. In the second most important criterion – “Heat inertia” – the blubber has the highest local priority. In general, this gives a significant advantage over other alternatives. Sensitivity analysis shows that the structure of the established *AHP* is sensitive to changes in the weight of criteria.

The results obtained using *AHP* method for choosing the best alternative of nature strategies to apply for innovative thermal envelope with climate adaptive properties will be further integrated in the next phases of biomimicry design spiral. Since blubber and blood circulation system has showed the greatest potential, these will be examined closer to discover mechanisms applicable to climate adaptive thermal envelope elements.

Blubber could serve as an inspiration in developing PCM containing structures that helps to deal with temperature fluctuations both inside and outside. Blood circulation system features could be integrated in PCM systems as well, optimizing the energy capture and release processes and to assist in adaption to changing conditions – the main task for blood circulation in living organisms.

*MCDM* method *AHP* can be successfully used in biomimicry approach. *AHP* hierarchy structure is useful in biomimicry design spiral phases – “biologizing the question” and “discovering natural models”. *AHP* helps to define criteria important to the goal and evaluate relative importance of every criterion in order to evaluate alternatives afterwards. The presented example of analytic hierarchy process used in biomimicry approach will serve as guidance for designers and researchers to evaluate biomimetic principles for practical application in the design of buildings – building envelope, energy production technologies, design of new generation building materials, etc.

## 1.6. Innovative climate adaptive solar energy storage element Bi-SES, emulating nature strategies

Following the results of the multi-criteria analysis, the properties of blubber and its role in the body are considered in the development of the innovative building envelope concept.

Formula  $M = h_{\text{cond}} (T_b - T_a) + h_{\text{conv}}(T_s - T_a) + h_{\text{rad}} (T_s - T_{\text{sur}}) + E + S$  that is determining the necessary metabolic exchange for an animal to compensate for all heat exchange processes served as an inspiration. Attention was drawn to the component S, heat storage. The study draws the boundary between the static “yesterday” and the dynamic “tomorrow” building envelopes that will take active part in the building’s energy cycle. Therefore, the heat storage component in animal’s metabolic balance gave an impulse to incorporate this process into the building envelope, creating a prototype for the wall that can participate in the energy balance of the building as an energy accumulator. In animal’s body, energy storage takes place in the subcutaneous fat layer – blubber – consisting of fatty acids, phase change materials and capable of storing energy. In the building, this function can be performed by phase change material.

Another important aspect is the location of the thermal insulation layer. If thermal insulation lies outside of the radiating surface, the body surface temperature below the coat is only a few degrees cooler than the core temperature. But if insulation layer lies on the inside, then the outer surface / skin temperature is at ambient temperature. For cetaceans, the composition of the blubber is not the same throughout its thickness and the temperatures are also different. The outer layer has a steep temperature gradient, but the inner layer is almost equal to the body temperature. Another example – the fat layer in a camel’s hump is not only a nutrient reserve but also protection against overheating in the heat of the day. Accumulation of solar energy in the hump reduces the heat benefits to the core of the body, while in the evenings excess heat is emitted to the surrounding environment [16].

Fur and feathering correspond to the traditional concept – insulating the building from the outside. But for marine animals, the heat insulation layer – blubber – is located inside the radiant surface. And unlike the outer thermal insulation layer, it is possible to include or exclude inner insulation layer from the heat exchange processes. The blubber layer is a common thermoregulation milestone for marine mammals living in an environment where temperature fluctuations are low. Considering all potential heat transfer processes, decision has been made to explore the use of phase change material advantages in the development of an innovative facade system.

The biggest disadvantage of traditional building envelope structures is their static properties and the inability to adapt to changing climatic conditions and changes in indoor microclimate parameters. Therefore, in order to add dynamic properties to the proposed facade system, an example of brittle star was studied. Brittle star changes the surface properties – a lens arrangement transmits the sun’s rays to the receiver and changes the surface colour as needed.

The main task of the proposed design is to capture solar energy at maximal possible amount, to store it in the phase change material and to release it to the indoor space. The planned energy flow is reflected (Fig. 1.2) as the energy storage process in favourable conditions.

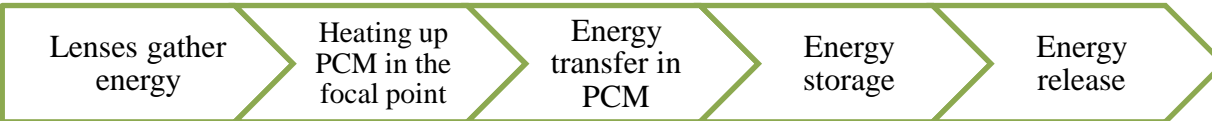


Fig. 1.2. Energy flow in Bi-SES.

## 1.7. Concept of innovative climate adaptive solar energy storage element Bi-SES

The developed solar facade module will be the medium between indoors and outdoors. The indoor temperature should be maintained within strictly defined comfort limits, while the outside temperature is variable. To introduce the ability to react to changes in outdoor temperature or in the indoor climate, there will be a permanent part – the phase change material and the dynamic parts – two thermal insulation layers with a very high thermal performance. One layer is located outside of PCM container (external thermal insulation layer), the other one – to the inside of PCM container (internal thermal insulation layer) (Fig. 1.3).

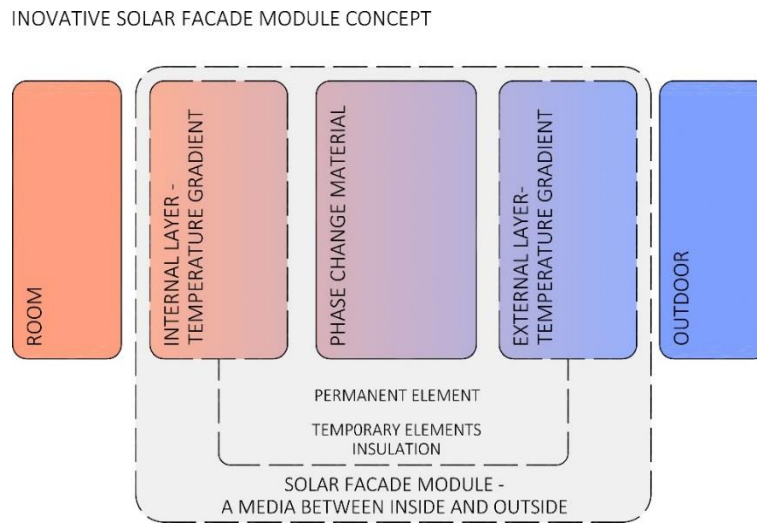


Fig. 1.3. Conceptual Bi-SES design.

The Solar Facade Module can be exposed to three different situations. When a module can be charged during the summer season under intense sunlight conditions (Fig. 1.4). The most intense sunlight in the summer is mostly in the middle of the day when the outdoor air temperature exceeds the indoor comfort temperature and additional solar heat gains are not desirable (to avoid the cooling). In such circumstances, the external thermal insulation layer is removed and solar heat is transferred into the phase change material. The PCM gradually heats up to a phase change state. During the phase change state, the material is transforming the physical state from solid to liquid, temperature is constant, and latent heat is stored (energy accumulation is taking place at this point). If there is enough solar energy at the end of the phase change, PCM temperature increases (sensible heat). Since the indoor room does not need heat (it is summer), the inner insulation layer performs its functions and prevents heat transfer into the room.

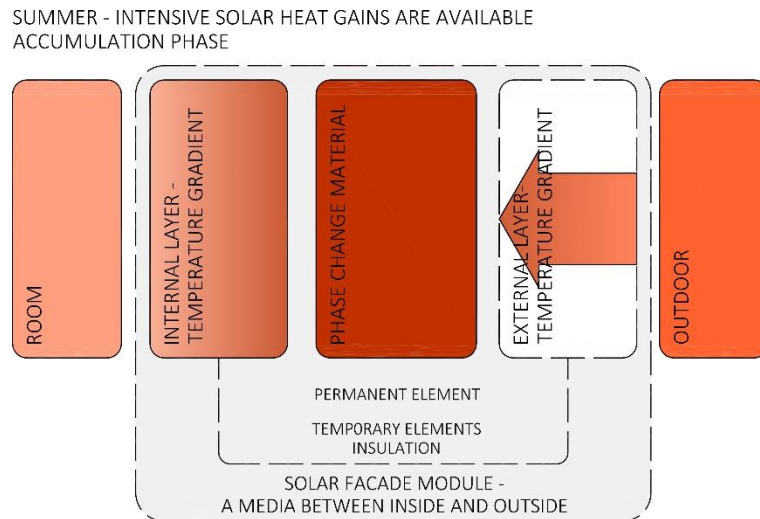


Fig. 1.4. Conceptual Bi-SES design – charging phase.

The next situation is the conditions of a summer evening / night / early morning, when there is no sufficient solar radiation for the southern facade and the outdoor air temperature is lower than the room temperature, which has fallen below the comfort requirements (Fig. 1.5). Such conditions are suitable for the energy release phase. The external heat insulation protects the PCM from heat loss outwards. The internal thermal insulation is removed and the heat from PCM, which at that time has a higher temperature than the indoor space, is transferred to the room (Fig. 1.5). First, sensible heat is transferred, then the phase change takes place at constant temperature – latent heat is released. When the temperature in the phase change material begins to fall below the indoor comfort temperature, the internal insulation layer covers the surface to reduce the total heat loss from the room against the outdoor environment. In between, i.e. at the moment when solar radiation is no longer available, but heat is not yet needed for the room, both layers of insulation isolate the phase change material from both sides – the indoor and outdoor spaces, preventing the cooling of phase change material.

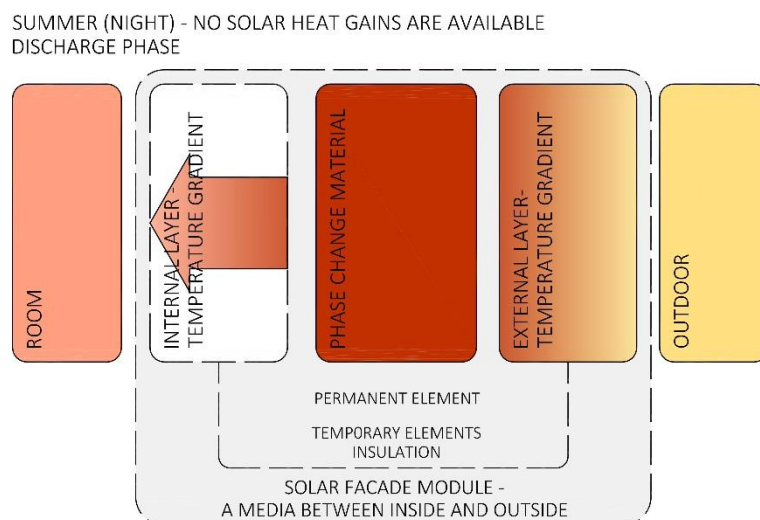


Fig. 1.5. Conceptual Bi-SES design – discharging phase.

The last major situation is winter conditions when solar radiation is available under very limited conditions. Outdoor air temperatures are significantly lower than the desired indoor temperature regardless of the time of day, and day or night. Such conditions are the passive phase of the solar facade module, where the possibilities to charge the phase transition material are minimal and the solar facade works as a thermal insulator with all the layers together to prevent conduction heat loss (Fig. 1.6).

The thermal insulation thickness to the outdoor space should be wider than to the indoor, because the potential temperature gradient between the phase change material and the outdoor environment will be significantly steeper than the gradient between PCM and indoor, especially in critical cold conditions – clear sky winter nights.

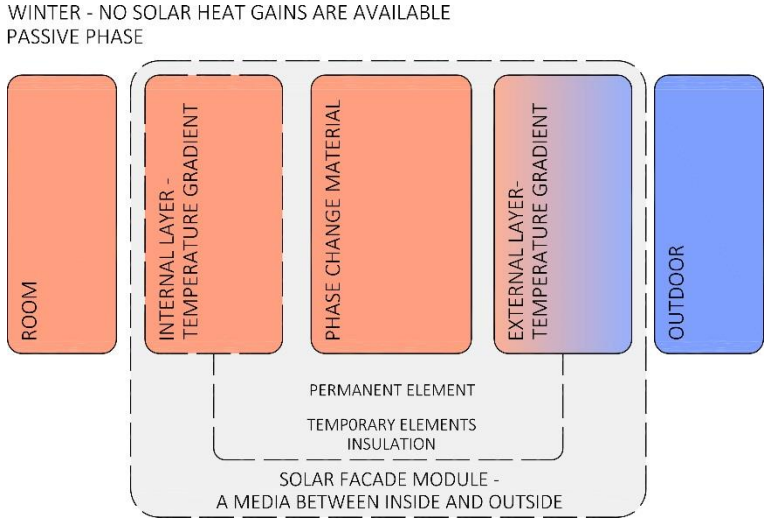


Fig. 1.6. Conceptual Bi-SES design – passive phase.

In thermoregulation systems in the nature, the ratio of the fat layer to the body core volume is significantly higher to provide the required energy reserve and thermal insulation. Building envelope makes up 5 % to 10 % of the total building volume depending on the size of the building. The aspects of thickening of the phase change material might be considered – the benefits of the energy balance against additional costs. An alternative would be to introduce a “circulatory system”, inspired by nature, for circulating circuits and accumulator tanks, for transferring heat from the PCM after phase shift (Fig. 1.7). Such a system should be equipped with valves that allow circulation, when the phase change material reaches a certain sensory heat limit and stops the circulation, reaching the phase change temperature. A more precise diapason for circulating activation and deactivation temperatures should be detected in a separate study.

In order to accelerate the capture of solar energy in the phase change material, the outer plane features the Fresnel lens, which, unlike a conventional lens, is compact and low in weight, which are important factors in building a new building element. Other heat exchange enhancer for PCM is metal elements incorporated in PCM container.

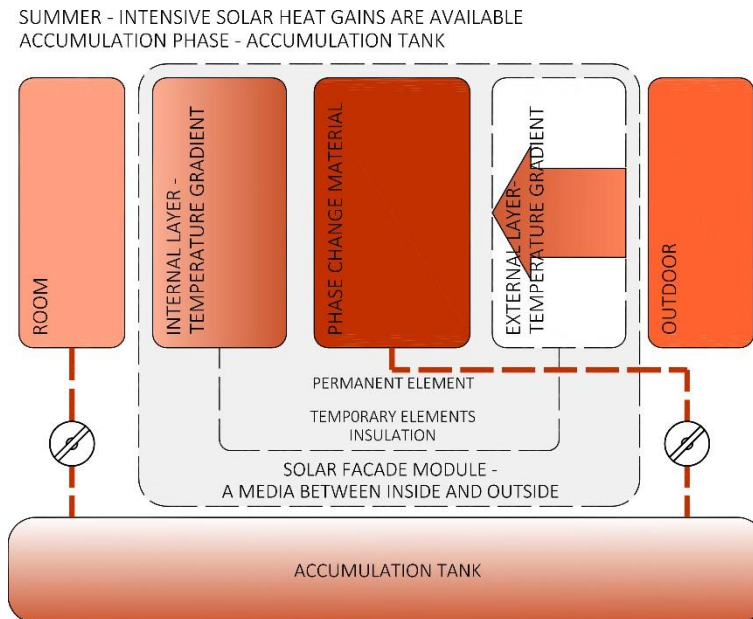


Fig. 1.7. Conceptual Bi-SES design – charging phase with accumulation tank.

The next steps to be taken in developing solar facade module Bi-SES are as follows.

1. To find the most suitable phase change temperature.
2. To find the most suitable PCM materials.
3. To design Bi-SES:
  - 1) define Bi-SES optimal dimensions;
  - 2) define PCM volume;
  - 3) choose PCM;
  - 4) choose heat exchange enhancers;
  - 5) choose Fresnel lens (focal distance, dimensions);
  - 6) choose optimal thermal insulation materials.
4. To build an experimental setup of Bi-SES prototype:
  - 1) design experimental set up that imitates indoor space and bordering wall;
  - 2) choose the location of experimental setup;
  - 3) define necessary measurements;
  - 4) install monitoring equipment.

## **2. EXPERIMENTAL RESEARCH OF CLIMATE ADAPTIVE BUILDING SHELL ELEMENT BI-SES**

The research consists of two experiments. The goal of the first experiment is to choose the most suitable phase change element for Bi-SES. The goal of the second experiment is to compare Bi-SES prototype with reference wall.

### **2.1. Experiment I. Choosing the phase change material: paraffin, salt hydrates, fatty acids**

Phase change materials that change the physical state from liquid to solid are more suitable for building components because they have relatively small volume changes in the phase change process compared to the phase change liquid-gaseous, gaseous-liquid. The most commonly used phase change materials in building products are paraffins and fatty acids from organic PCMs and salt hydrates from inorganic compounds. The aim of the first part of the experiment is to determine the most suitable phase change material for energy storage in the solar facade module Bi-SES. All three groups are studied in this research (see full version) and products chosen to be used in Bi-SES.

#### **2.1.1. Heat transfer enhancers in phase change materials**

Most phase change materials have low thermal conductivity. This makes heat capture and release processes inert. Therefore, composite materials with phase change materials for the latent heat storage are supplemented with significantly higher thermal conductivity elements to accelerate heat transfer and ensure faster phase change. The most commonly used thermal conductivity enhancers in phase change materials can be divided into two conceptually opposed groups. The first is to include PCM microcapsules in higher thermal conductivity materials. The second approach is to place higher and very high thermal conductive materials – metals, graphite, carbon materials in phase transition material.

#### **2.1.2. Phase change materials used in the experiment**

One of the tasks of the study is to select the most appropriate phase change material for Bi-SES. In the course of this study, it is defined that the facade module requires phase change material with a melting temperature of  $\pm 22$  °C. To cover all most commonly used groups, the following materials have been selected: RT21HC (paraffin), SP21E (salt hydrates (Rubitherm)). Salt hydrates must be kept at 0 °C for 24 hours before use. In this experiment, salt hydrates were held in the JEIOtech TH-G temperature and humidity chamber.

A eutectic mixture (palmitic acid ( $\geq 98.0$  %) and capric acid ( $\geq 98$  %) (Labochema)) has been produced to obtain fatty acid with the required properties, and a procedure has been performed to verify the thermal properties of the material obtained [17], [18]. The melting temperature of palmitic acid is 59.4 °C and of the capric acid it is 32.14 °C. Both fatty acids were dissolved in liquid phase and mixed with a mass ratio of 76.5 : 23.5. Melting temperature has been established in a water bath containing temperature sensors. When the temperature does

not change, PCM starts to accumulate heat. Figure 2.1 shows the experimental setting with a flask filled with a mixture, and two thermocouples are added to it. One thermocouple is in the centre while the other is closer to the edge of the flask. The third thermocouple measures the water temperature. Thermocouples are marked with red arrows. Table 2.1. reflects the thermal properties of fatty acids used for the eutectic mixture.



Fig. 2.1. Eutectic mixture in constant temperature water bath with thermocouples.

Table 2.1

Properties of Used Fatty Acids and Prepared Mass Fraction [19], [20]

<b>Fatty acid</b>	<b>PA</b>	<b>CA</b>	<b>Unit</b>
Specific heat solid	1.9	1.9	kJ/(kg K)
Specific heat solid	2.1	2.8	kJ/(kg K)
Density solid	989	1004	kg/m <sup>3</sup>
<i>w</i> l%	23.5	76.5	%
<i>m</i> <sub>e</sub>	600		g
<i>m</i> <sub>fi</sub>	141.0	459.0	g

Before the experiment, the eutectic mixture was chilled to 0 °C. The water temperature was 40 °C; the actual temperature was lower around the flask, because the water bath did not have a lid or any other type of insulation to prevent heat loss. This experiment shows the typical behaviour of PCM. Middle zone coloured with red dashed lines in Figure 2.2, is the latent heat phase when the mixture melts.

The results show that the temperature range for both thermocouples is almost identical until melting and during the melting phase. After the phase change, switching to the sensible heat storage, there are significant differences in the temperature areas at the edge of the flask and in the middle, explained by the low thermal conductivity of the material.

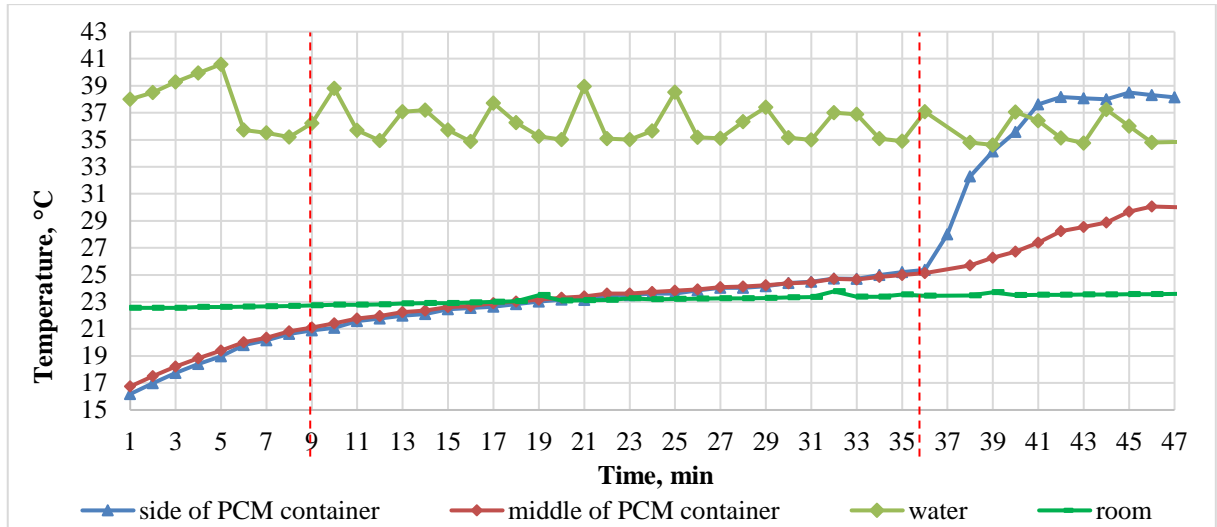


Fig. 2.2. The melting point for CA:PA eutectic.

The eutectic mixture was observed in both phases, no volume changes were detected. Density was calculated  $\rho = m / V = 911.64 \text{ kg/m}^3$ . The melting temperature range was 21 °C to 25.4 °C (Fig. 2.2), the temperatures were measured with thermocouples every 5 seconds and the average temperature was measured every minute. The results show that this mixture has the same characteristics as those described in the literature [20]. The specific calorific value for the eutectic mixture is in the liquid phase  $c_{eu} = 1.9 \text{ kJ}/(\text{kg K})$  and for the solids  $c_{eu} = 2.64 \text{ kJ}/(\text{kg K})$ . Table 2.2 summarizes the characteristics of the PCM used in the experiment.

Table 2.2

Properties of PCMs Selected for the Experiment. RT21HC, SP21E [21]

Property	PCM			Unit
	RT21HC	SP21E	CA:PA [20]	
Melting temperature.	20–23	22–23	23.12	°C
Freezing temperature.	21–19	21–19	22.15	°C
Heat storage capacity $\pm 7.5 \%$ .	190	160	–	kJ/kg
Latent heat storage of melting.	–	–	156.44	kJ/kg
Latent heat storage of freezing.	–	–	150.29	kJ/kg
Combination of latent and sensible heat in a temperature range of 13 °C to 28 °C.	53	44	–	Wh/kg
Specific heat capacity.	2	2	–	kJ/(kg K)
Density of solid, at 15 °C.	0.88	1.5	911.64	kg/l
Density of liquid, at 25 °C.	0.77	1.4	–	kg/l
Heat conductivity (both phases).	0.2	0.6	–	W/(m K)
Volume expansion.	14	3–4	1	%
Flash point (PCM).	140	–	–	°C
Max. operation temperature .	45	45	–	°C

### 2.1.3. Construction of an experimental setup

In order to compare three different phase change materials, three test boxes are created on the experimental setup, each PCM has its own box. Each box is composed of three parts. Part 1 “thermal shell” is a plywood box lined with a 20 cm mineral wool (Fig. 2.3). Outer dimensions of the box are 55.7 cm  $\times$  55.7 cm  $\times$  60.7 cm. Part 2 is a room in the box simulating a well-

insulated indoor space exposed to the outdoor climatic conditions. Part 3 is the “solar facade module Bi- SES” composed of commercially available materials and comprising a variety of components (Fig. 2.3). All the materials used were selected to withstand high heat loads, given that concentrated solar power can heat the panel up to 200 °C. The following materials were used:

- 4 mm glass for the PCM container;
- aluminium fittings for the geometric stability of the container;
- sealing material – silicone – to ensure airtight container construction; the sealing material selected must ensure high temperature strength and ensure that the chemical composition of the sealing material is resistant to the effect of each PCM.
- phase change material – RT21HC, SP21E, CA : PA;
- copper plate of 1.5 mm thickness, copper bars  $\varnothing$  5 mm, solder;
- folded aluminium sheet;
- triple glazing;
- mineral wool.

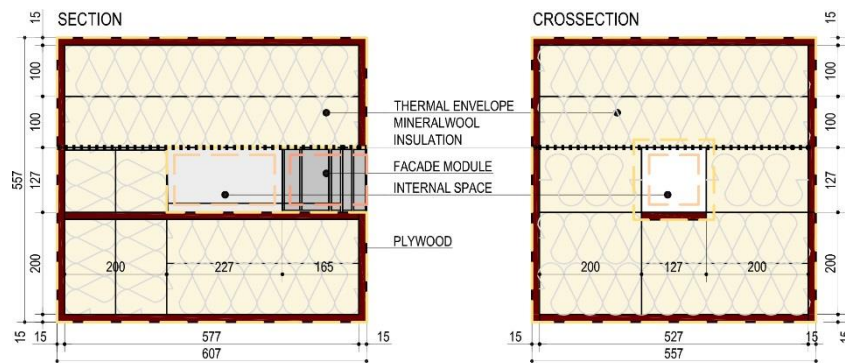


Fig. 2.3. Test box with Bi-SES sections (dimensions, mm).

After the PCM chamber has been created and tested for density, it can be filled with the liquid FPM. During the filling process, the FPM must be uniform in order to avoid the formation of air pockets in the solid.

There is a Fresnel lens in the outer layer of the module (Fig. 2.4). Its focal distance is 7.1 cm, the lens’s effective diameter is 101.6 mm, focal point area is 9.6 mm<sup>2</sup>, and light permeability 0.92. It is made of a polymethyl methacrylate [22].

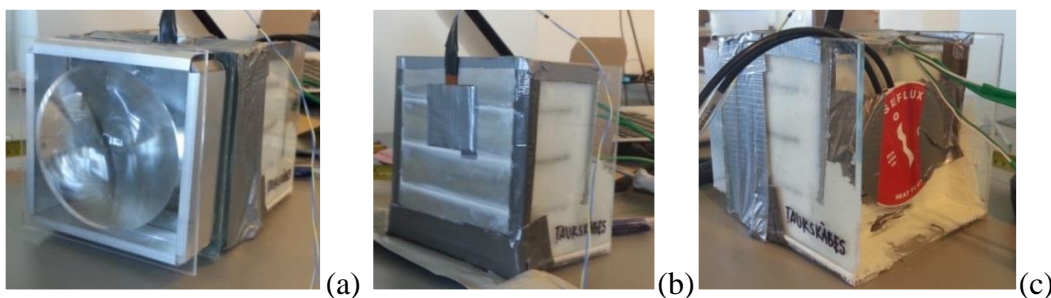


Fig. 2.4. (a) Fresnel lens integrated in Bi-SES; (b, c) heat flux sensors.

Metal heat transfer enhancers are used to accelerate heat transmission in phase change material (Fig. 2.5 (b)). A copper plate (119 mm x 113 mm) with copper bars (346 W/(m K); 0.031 m<sup>2</sup>) is used for salt hydrate and paraffin (Fig. 2.5 (a)). 25 copper bars, of a diameter of 5 mm, are attached to the plate at 20 mm from each other. Folded aluminium sheet with three 45 mm deep shelves for surface augmentation (226 W/(m K), 0.046 m<sup>2</sup>) is used for the eutectic mixture. Plates are hermetically attached to a glass container with silicone.

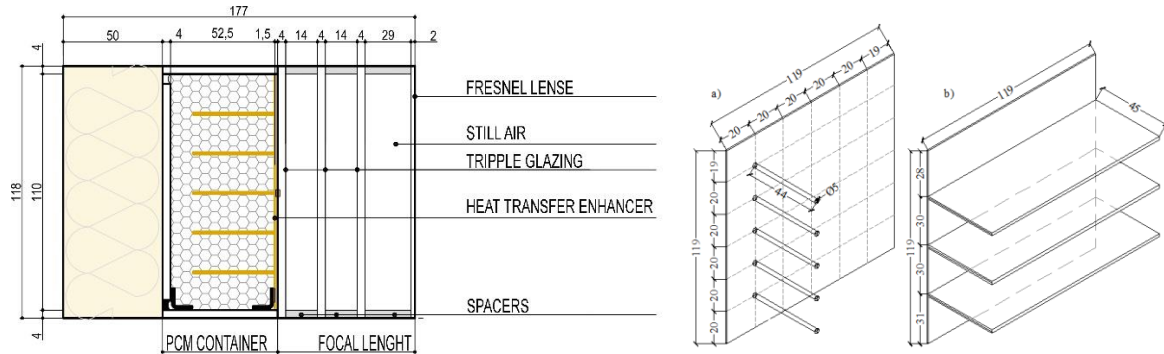


Fig. 2.5. Bi-SES cross section (right) and heat enhancers (left).

Metering equipment is installed in the test box to control the processes inside the FPM chamber and in the room. The measuring instruments selected and a simplified experimental setup diagram are shown in Figure 2.6 and described as follows.

1. Thermocouples with data recording equipment CR1000 ± (0.06 % reading + offset) are used for indoor and outdoor temperature measurements. Temperature measurements are recorded every 30 seconds.
2. Solar radiation flow is measured by the Kipp & Zonen CMP3 pyranometer.
3. Thermocouples have data recording equipment CR1000 ± (0.06 % reading + offset). Each PCM chamber has 3 thermocouples.
4. The heat flow meter Sequoia SHF is located on the outer surface of the PCM chamber and Huseflux HFP01 is located on the inner surface of the PCM chamber.

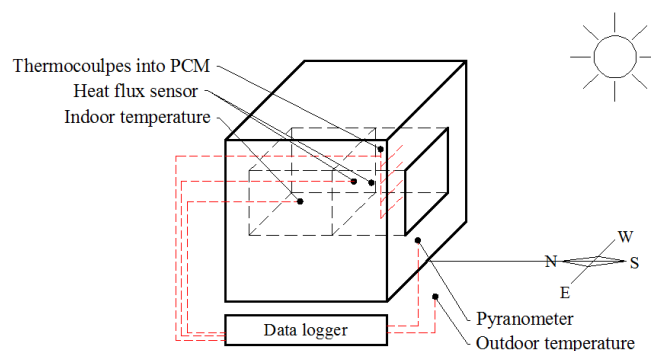


Fig. 2.6. Metering equipment scheme.

### 2.1.4. Comparing the performance of three phase change materials

Three boxes with elements of solar facade module Bi-SES were installed under real climatic conditions, with the lens facing south. Geographical coordinates of the experimental setup were 24°04'48.7" East longitude and 56°57'03.0" North latitude. The boxes are numbered in the order

they were installed (Fig. 2.7). In each test box different phase change material is used in Bi-SES: 1) Box 1 (K1) – eutectic mixture of fatty acids with aluminium ribs, without heat source in the room; 2) Box 2 (K2) – paraffin RT21HC with copper plate and copper rods, heat source (+22 °C); 3) Box 3 (K3) – salt hydrate, with copper plate and copper rods, heat source (+22 °C);

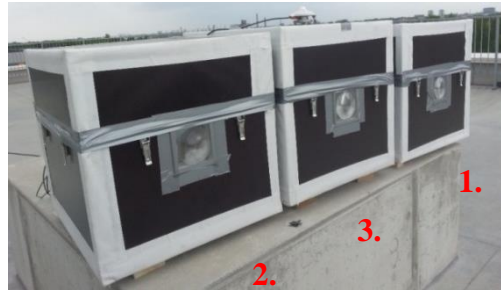


Fig. 2.7. Bi-SES under real climatic conditions.

### 2.1.5. Results of phase change material selection experiment

Figure 2.8 shows the results of experimental measurements done from 24.05.2015, 0:00 to 27.05.2015, 23:59. The graph shows outdoor air temperature, solar radiation, and temperature in each of the phase transition materials. K1, K2, K3 denote experimental stands.

All boxes were placed in outdoor conditions before 24.05.2015. The first two days were sunny with solar radiation over 1000 W/m<sup>2</sup>. The third day was cloudy with a maximum solar radiation of 400 W/m<sup>2</sup>. The fourth day was partly cloudy with low radiation levels 250–400 W/m<sup>2</sup>. Outdoor air temperature on sunny days was from 7–10 °C at night and up to 18–21 °C during the day. On cloudy days, the outdoor air temperature variation is lower, i.e. from 10 °C at night to 15 °C during the day.

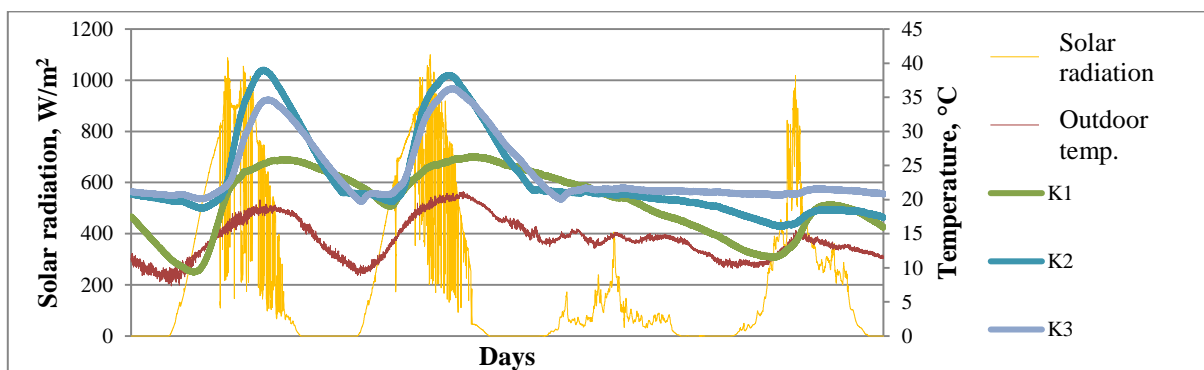


Fig. 2.8. First part of the experiment – selection of phase change material 24.05.–27.05.

In K2-RT21HC and K3-SP21E boxes with heating elements (Fig. 2.8) the temperature in phase change materials is rising with a slight time lag comparing to the increase in solar radiation. K2-RT21HC reaches the temperature that is 3–5 °C higher. In both PCM containers, the transition from the latent heat phase to the sensible heat happens very quickly. After solar radiation decrease, with a slight time lag, the temperature in PCM containers lowers. On the third, highly cloudy day, the heating element keeps a steady temperature in PCM. On the fourth, semi-cloudy day, temperatures in PCM are slightly rising.

From 24.05.2015, 0:00 to 25.05.2015, 23:59 two full charge-discharge cycles are visible (Fig. 2.9). At first reaching the sensible heat phase quickly during the day and afterwards gradually losing sensible heat during the night and moving into the latent heat discharge phase. Paraffin reaches higher temperatures, while salt hydrate returns heat more slowly.

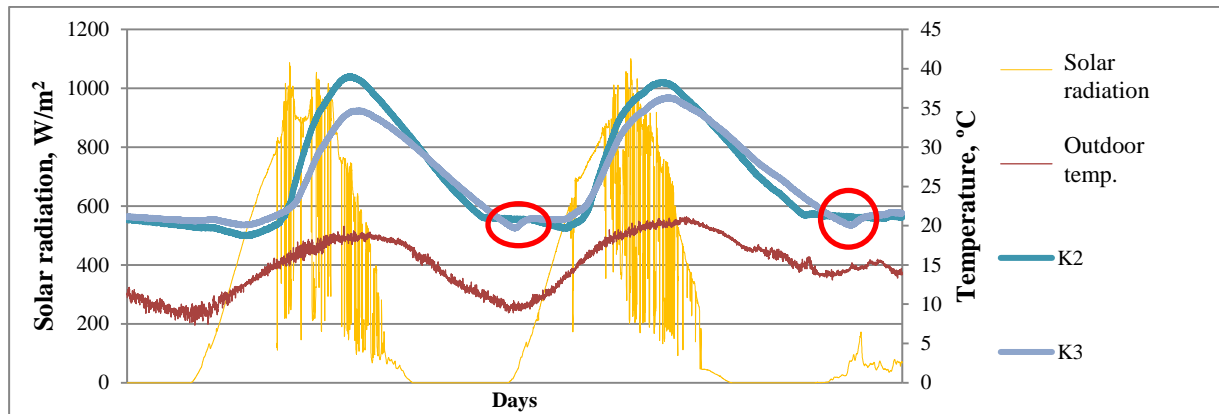


Fig. 2.9. Paraffin and salt hydrate charging / discharging cycles.

Figure 2.9 reflects the supercooling phenomenon in salt hydrate (red). The PCM temperature prior to the solidification phase decreases below the described solidification temperature. The solidification temperature is 19–21 °C. At first, the temperature in salt hydrate falls to ~19.5 °C and then stabilises at ~21 °C. The experiment does not show such temperature variation in paraffin.

Two charging-discharging cycles are observed in K1-CA:PA from 03.06.2015, 0:00 to 05.06.2015., 17:33 (Fig. 2.10). In the first hours of 03.06, the PCM is cooling down. Solar radiation activates at 4:23. The PCM temperature starts to rise with a 2 h shift. Between 9:13 and 11:45, a reduction followed by fast increase in solar radiation can be seen in the graph. The latent heat phase very rapidly alters into sensible heat and is not noticeable in the graph. In 04.06. and 05.06. there is a short steady temperature in the melting temperature zone of the eutectic mixture. During the cooling phase no solidification phase is observed. This may be related to the ratio of PCM volume to heat transfer enhancers, which is a significant source of heat loss during the solidification phase of the PCM.

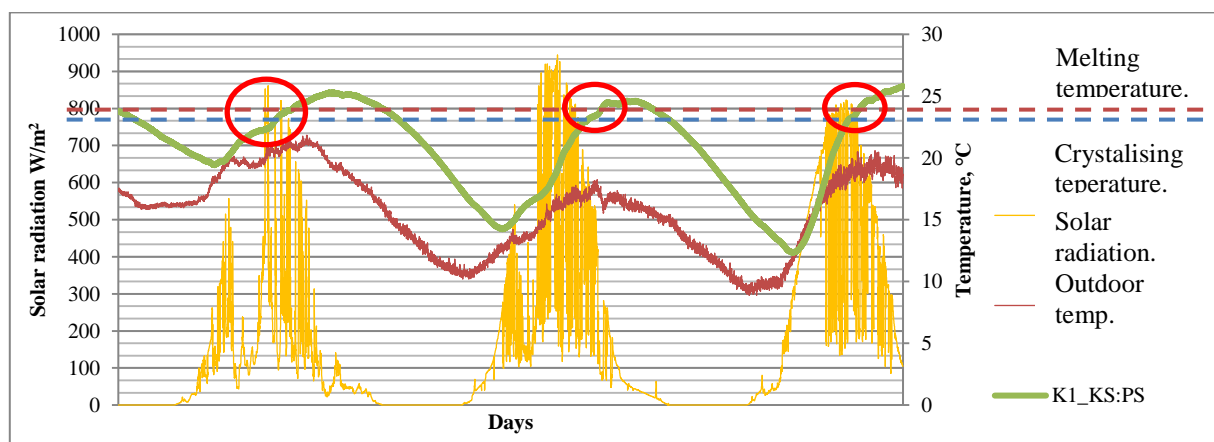


Fig. 2.10. Charging-discharging cycles in eutectic mixture (CA:PA).

In Figure 2.11 the positive values in the heat flow graph reflect the direction from sun radiation to PCM (red curve). The negative values of the curve show heat losses from the PCM outwards. For heat flow on the inside surface of the PCM container, the positive values of the blue curve reflect the heat flow from PCM to the room; the negative values reflect the heat flow from room to PCM. The blue curve section with a value of  $\sim 0$  (C) reflects the situation after a cloudy day when the temperature in the phase change material is equal to the indoor temperature and the heat flow does not occur. In the night between 22.05. and 23.05., the heat flow in the PCM goes in both directions, as marked with A. Heat flow in zone A occurs during the night. Heat losses outwards are the negatives of the red curve. The blue curve shows that certain heat is flowing to the room. During the day there is a heat energy flow to room B as well.

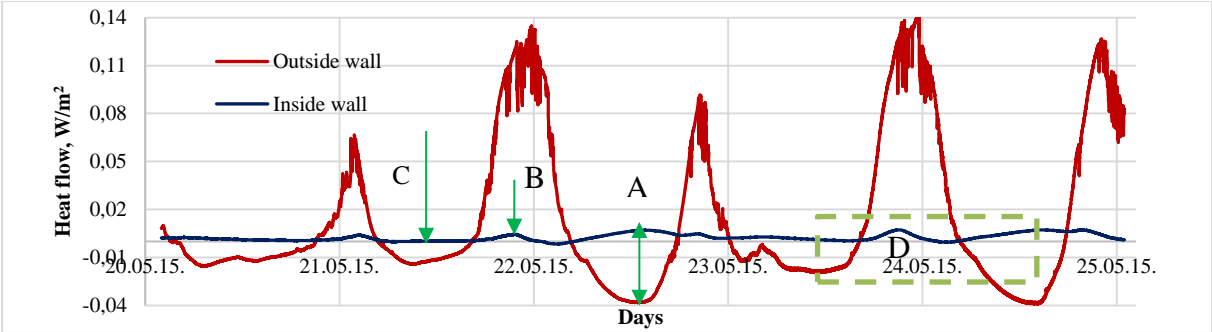


Fig. 2.11. Heat flux in test box K1-CA:PA.

Zone D corresponds to sunny day (24h) in 24.05.2015, the red curve reflects the heat gains in PCM from solar radiation during the day and heat losses during the night. The blue curve has two peaks of positive values. The first is when the PCM is warmed up and the indoor temperature is lower than the PCM temperature. The second peak appears at night when solar radiation is not available. The indoor space begins to cool, but the temperature in the PCM is higher than the indoor temperature – the heat from PCM is transferred to the room.

Measurements of K2 and K3 cannot be directly compared to K1 results due to the conditions. The boxes contain heating elements. The heat flow on the outer surface of the PCM is similar to the situation in test box K1 – the positive values of the red curve reflect the warming of PCM, but the negative values – heat losses (Fig. 2.12). The heat flow on the inside surface of the PCM container differs. The negative values of the blue curve reflect the situation when the PCM is heated from the room, due to the heating element, which prevents the temperature from falling below 22 degrees. Thus, the indoor temperature is higher than the PCM temperature.

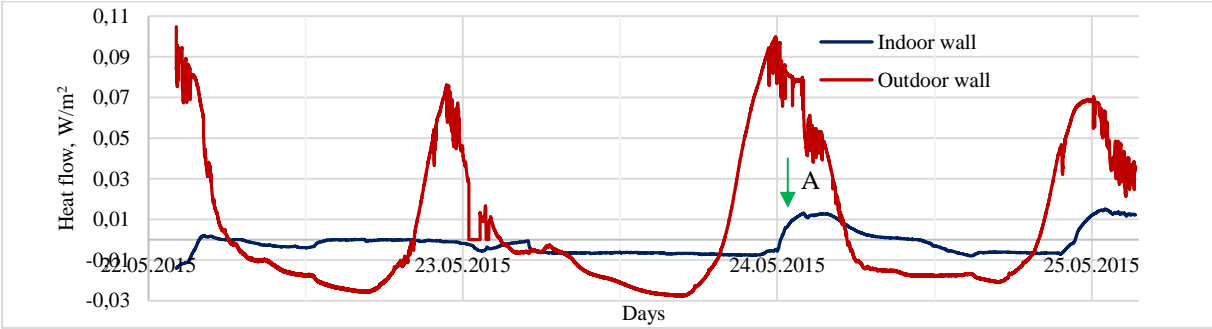


Fig 2.12. Heat flux in K2-RT21HC.

Despite heating the PCM from indoors, there is also a discharge of heat to the room after intensive sun radiation (indicated by A, Fig. 2.12).

### **2.1.6. Conclusions from the phase change material selection experiment**

From the results of the first part of the experiment, it is concluded that paraffin K2-RT21HC is the most effective, because, first, the highest temperature in the sensible heat zone is observed, secondly, there is no super-cooling phenomenon observed, thirdly, it shows the best compatibility with other materials used such as the heat transfer enhancer, plastic parts, and the binders. Therefore, the second part of the experiment, which studies the performance of the solar facade module Bi-SES and compares it with the reference wall, uses paraffin RT21HC.

In addition to the conclusions on the selection of the most suitable phase change material, ideas how to improve the Bi-SES module are gained in order to reduce the outdoor heat loss via heat transfer enhancer. It enhances the heat flow in both directions – to the PCM in sunny days and outwards during the absence of the sun radiation.

## **2.2. Experiment II. Comparison of Bi-SES with the reference wall**

### **2.2.1. Construction of Bi-SES-II**

In the second part of the experiment, a comparison between the facade module and the reference wall was made. The geographical location and trial boxes are identical to those in the first part of the experiment (see section 2.1.3). Prior to starting the experiment, the original facade module was optimized, reducing heat loss to the outside. Triple- glazing in the focal space of the lens is replaced with focusing chamber in the form of a cone according to the lens focusing geometry (Fig. 2.13). The cone for aerogel filling is built from the self-hardening modelling clay *DAS*. There is still air in the cone compartment. The space between the cone and the copper plate is filled with aerogel granules LA1000 (Cabot) (low thermal conductivity and high solar energy permeability) to reduce thermal losses from the copper plate. The experimental solar facade module is built from commercial materials and consists of : PCM - RT21HC paraffin (Rubitherm Technologies GmbH); modelling mastic *DAS*; aerogel.

PCM is filled in a container that corresponds to the outer dimensions of the lens (119 mm × 110 mm × 47.5 mm). Paraffin properties are given in Table 2.3 PCM does not fill 100 % of the container due to varying volume of the material in different physical states. One wall of the container is the copper plate with enhancers while the other walls are made of 4 mm glass. Total U-value for solar facade module is 0.22 W/(m<sup>2</sup>K) and for reference wall is 0.28 W/(m<sup>2</sup>K).

Thermophysical Properties of Paraffin [23]

Parameter	Value	Parameter	Value
Specific heat capacity solid/liquid, kJ/(kg K)	2	Latent heat of fusion, kJ/kg	190
Melting temperature, °C	20–23	Density solid/liquid, kg/m <sup>3</sup>	0.88/0.77
Solidification temperature, °C	21–19	Volume change, %	
Thermal conductivity solid/liquid, W/(m K)	0.2		

### 2.2.2. Monitoring equipment

Instrumentation scheme of monitoring equipment is presented in Fig. 2.13. It includes monitoring of indoor temperature, outdoor temperature, solar radiation, temperature in PCM in three layers, and heat flux on the external surface of copper plate and indoor side of PCM container. Solar flux data are measured with pyranometer with accuracy  $\pm 10 \text{ W/m}^2$  or 5 % from the reading. Outdoor and indoor temperatures are measured with K type thermocouples with accuracy  $\pm 1.1 \text{ }^\circ\text{C}$  or  $\pm 4 \%$  of the reading from  $0 \text{ }^\circ\text{C}$  to  $1250 \text{ }^\circ\text{C}$ , and  $\pm 2.2 \text{ }^\circ\text{C}$  or  $\pm 2 \%$  of readings from  $-200 \text{ }^\circ\text{C}$  to  $0 \text{ }^\circ\text{C}$ . Heat flux is measured with Sequoia heat flux plates. All measurement data are saved in a Campbell Scientific CR1000 data logger. 1-minute time steps for all measurements are taken.

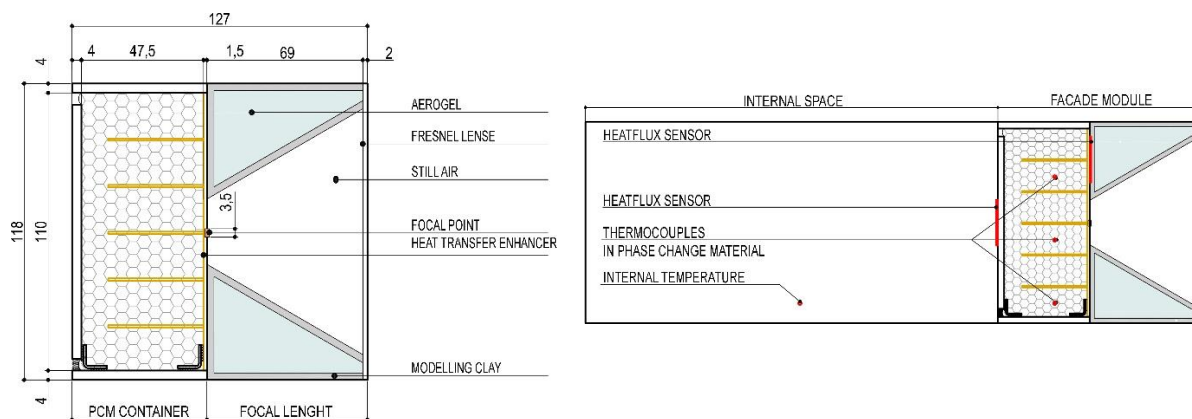


Fig. 2.13. Cross-section of Bi-SES (left). Instrumentation scheme of monitoring equipment (right).

### 2.2.3. Experiment II

In the experimental study, two test boxes located side by side with and without facade module were monitored during September 2017. Both test boxes were placed on the roof of the building and exposed to identical boundary conditions. Test boxes were faced South and were shaded from all other sides (Fig. 2.14). The solar tracking was done manually by turning the platform below both boxes.

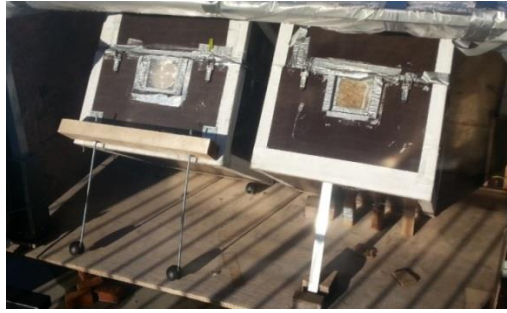


Fig. 2.14. Experimental test box with the facade module (left) and the reference box without facade module (right).

Both boxes were instrumented to monitor the outdoor climate, indoor temperature, heat transmission through the building envelope, and temperatures in the phase change material. Data gathered during monitoring period were analysed and used to calibrate the simulation model, which was used to perform annual and seasonal energy balance assessment. Longitude of the experimental site is 24°04'48.7"E and latitude is 56°57'03.0"N.

#### 2.2.4. Results and analysis

Heat fluxes and temperatures measured within and on both sides of the module for one day (25 September 2017) are presented in Figure 2.15. The graph starts at midnight when the solidification of PCM generates latent heat, which causes heat flux to both indoors and outdoors. The flow from PCM to outdoors is higher than to indoors due to higher temperature difference. When the sun starts rising at 7:05, heat flow from outdoors to PCM changes direction and becomes positive at 9:05. Meanwhile, heat flux to room starts to fall and then increase again at 13:30. When the solar radiation decreases at 13:22, so does the heat flux to PCM until it becomes negative at 16:55, i.e. heat losses from the module to outdoors. During the night, solidification of the PCM starts when the latent heat is released at about 23:40 and both heat flux to indoors and outdoors increases. However, indoor temperature falls because heat flow to outdoors dominates over heat flow to indoors.

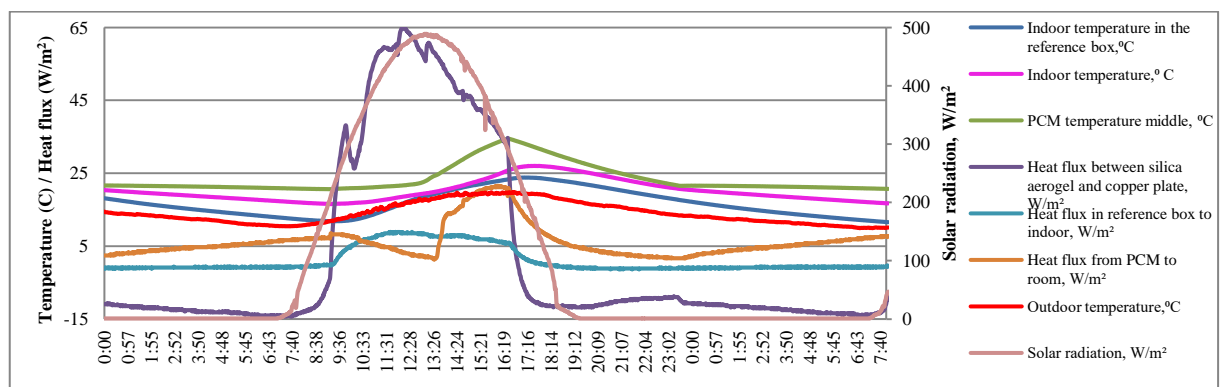


Fig 2.15. Heat fluxes, solar radiation and temperatures measured in the reference box, and the module on 25 September 2017.

The main driver behind the dynamics of the heat flux from PCM to room is the temperature difference between PCM and the room temperature. During the night, while the latent heat is released during solidification process starting at 23:40 and ending at 7:55, PCM temperature is

almost constant but room temperature falls, thus the temperature difference increases. Heat flux from PCM to the room increases due to both effects: latent heat and temperature difference. PCM temperature starts to increase after the heat flux from solar radiation enters PCM at 9:05 and melting of PCM starts. At the beginning of this process the temperature difference is decreasing leading to reduced heat flux, while afterwards the temperature difference is increasing due to a delay caused by PCM melting process. At 13:30, heat flux starts to decrease because the room temperature is getting closer to PCM temperature. During the night, the solidification process starts at 23:40 when PCM reaches solidification temperature.

Dynamic behaviour of the room temperature and heat flux in the reference box differs from the same parameters measured in the module. Heat flux in the reference box coincides with the delayed solar radiation and at its maximum peak, which is reached at 11:50, is around four times less than in the module. The room temperature in the reference box differs from the module between 0.5 °C during the day reaching this value at 14:30 and 5 °C during the night at 7:50, which shows the impact of the thermal energy accumulation in the PCM.

The time lag between the solar radiation and PCM temperature is 3.5 hours, while between the PCM temperature and indoor temperature it is 45 minutes. In the reference box indoor temperature peak is delayed from the solar radiation peak by 4 hours.

Figure 2.16 illustrates the solidification process of PCM, which starts at 23:40. The temperature falls and then starts to rise. This is caused by the solidification process when PCM is starting to release latent heat and heat flux increases. Heat cannot be evacuated immediately, thus the PCM temperature is rising leading to supercooling. Heat flux increases more rapidly to outdoors than to indoors due to higher temperature difference between PCM and outdoors. When the heat flux to room starts to increase, the solidification temperature stabilizes around +21.6 °C. Solidification does not occur at the melting point and it is well illustrated by the hysteresis effect of PCM.

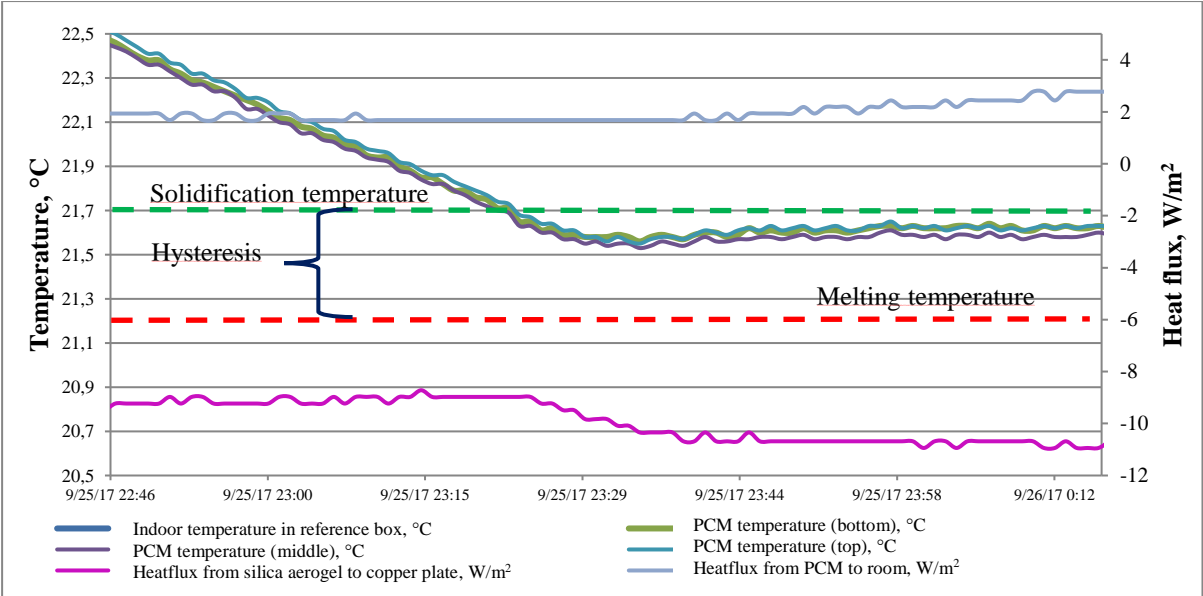


Fig. 2.16. Solidification process of the PCM.

### 3. MATHEMATICAL MODELLING OF CLIMATE ADAPTIVE MODULE BI-SES-II

#### 3.1. Mathematical modelling in *COMSOL Multiphysics*, heat transfer processes, boundary conditions

The experimental facade module was modelled in three dimensions in *COMSOL Multiphysics 5.1.*, simulating heat transfer considering heat conductivity, convection and radiation [24]. Time dependent study is applied for the model to compute temperature changes over time. The following boundary conditions are selected (marked blue in Figure 3.1 and Figure 3.2).

1. Heat transfer in solids (Fig. 3.1 (a)) –the relationship between the heat flux field  $q$  and the temperature gradient  $\nabla T$  in  $q = -k\nabla T$ .
2. Heat transfer with phase change (Fig. 3.1 (b)) – middle domain (50 mm).
3. Heat transfer in fluids (Fig. 3.1 (c)) – applied for air volumes;
4. Thermal insulation (Fig. 3.1 (d)) – this boundary condition assigns adiabatic condition. There is no heat transfer to / from these surfaces.
5. Heat source (Fig. 3.2 (a)) – solar radiation ( $\text{W}/\text{m}^2$ ). Solar radiation imitating Fresnel lens focus is concentrated in one spot ( $0.5 \text{ cm} \times 0.5 \text{ cm}$ ) as a heat load spot marked with red arrow. Solar radiation data corresponds to the average climate data in Riga.
6. Temperature (Fig. 3.2 (b)) – applied to the outer surface, outdoor temperature data corresponds to the average climate data in Riga.

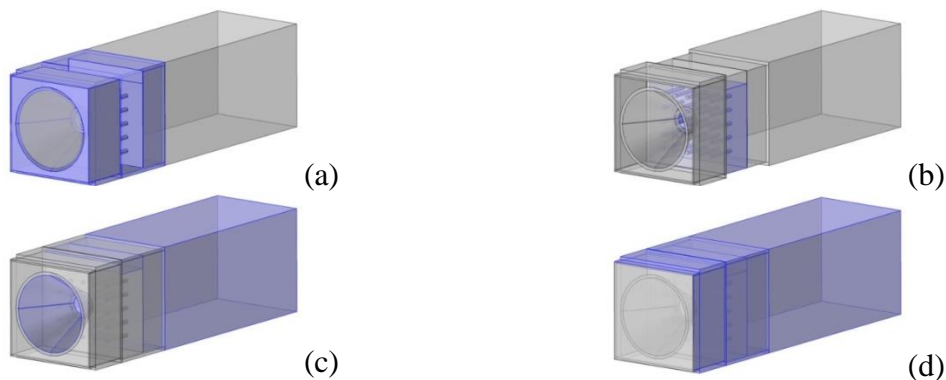


Fig. 3.1. Boundary conditions (respective volume is marked blue).

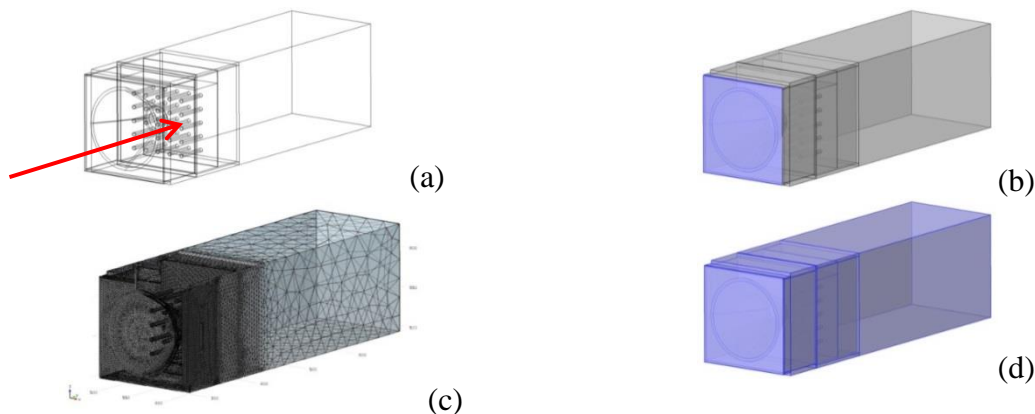


Fig. 3.2. Boundary conditions (respective volume is marked blue).

Heat transfer in solids was used in *COMSOL* for the outer shell of module (plywood and insulation). Outer surfaces face outdoor climate. Physics-controlled mesh size with finer elements was used. Time step was 1 h.

Initial temperature is the same for all components. Four simulations are made for typical Latvia climate seasons and corresponding outdoor temperature applied to the model.

### 3.2. Numerical study

The thermophysical properties of all materials are used as given in Section 2.1. The solar facade module is described as a time dependent, three-dimensional heat transfer problem coupled with phase change. A general form of the equations governing the heat transfer process in the solid and air sections of the module is described as follows:

$$\rho C_p \frac{\partial T}{\partial t} + \rho C_p u \nabla T - \nabla(k \nabla T) = Q, \quad (3.1)$$

where  $\rho$  – density, kg/m<sup>3</sup>;

$C_p$  – heat capacity, kJ/(kg K);

$k$  – thermal conductivity, W/(m K);

$T$  – absolute temperature, K;

$t$  – independent variable for time;

$Q$  – heat sources other than viscous heating, W/m<sup>3</sup>.

Phase change equations assume that there is no mixing in the liquid phase and the conduction equation in solid phase is the same as Equation 3.1. When PCM reaches its phase change temperature, it is assumed that it takes time between  $T_{PC} - \Delta T/2$  and  $T_{PC} + \Delta T/2$  ( $\Delta T$  is the transition temperature of PCM). The phase of the PCM during this period is defined by the function  $\theta$ , which represents the fraction of phase before the phase transition and is equal to 1 before  $T_{PC} - \Delta T/2$  (PCM is in solid state) and equal to 0 after  $T_{PC} + \Delta T/2$  (PCM is in liquid state). The temperature dependent density is calculated as

$$\rho = \theta \rho_{\text{phase1}} + (1 - \theta) \rho_{\text{phase2}}, \quad (3.2)$$

where indices phase 1 and phase 2 represent solid and liquid phases of PCM.

The specific heat capacity  $C$  is calculated as

$$C_p = \frac{1}{\rho} (\theta \rho_{\text{phase1}} C_{p,\text{phase2}} + (1 - \theta) \rho_{\text{phase2}} C_{p,\text{phase1}}) + L \frac{\partial a_m}{\partial T}, \quad (3.3)$$

where  $L$  – latent heat, J/kg;

$a_m$  – mass fraction:

$$a_m = \frac{1}{2} \cdot \frac{(1-\theta)\rho_{\text{phase2}} - \theta\rho_{\text{phase1}}}{(1-\theta)\rho_{\text{phase2}} + \theta\rho_{\text{phase1}}}. \quad (3.4)$$

Thermal conductivity is

$$k = \theta k_{\text{phase1}} + (1 - \theta) k_{\text{phase2}}. \quad (3.5)$$

### 3.3. Simulation output

COMSOL Multiphysics 5.1 provides output measurements for each dependent variable. To compare the results of the experiment with the simulation results and summarize conclusions, the temperature of PCM and the indoor temperature were selected as output data (Fig. 3.3).

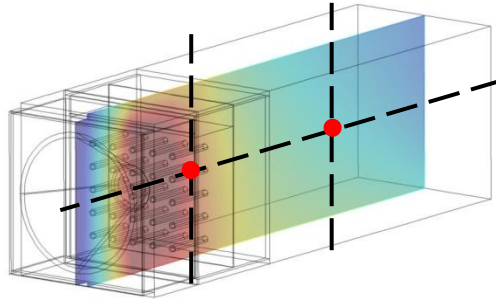


Fig. 3.3. Output data. PCM temperature, room temperature.

### 3.4. Validation of simulation model

Experimental data were compared to modelled results of 25 September 2017. Figure 3.4 shows a good agreement between simulation and measurements. The observed PCM temperature increases with smaller rate during melting process and increases faster after melting process has finished. The same trend is for room temperatures. The difference here is probably due to the transition temperature of PCM, which should be 1 °C instead of 3 °C, assumed thermal resistance of the external air layer, internal relative humidity, which is assumed to be 70 %.

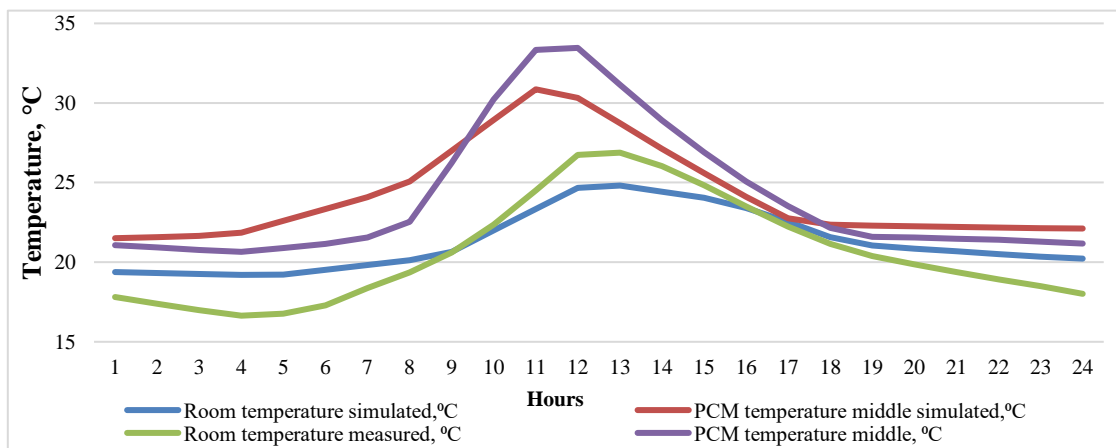


Fig. 3.4. Comparison of the measured and simulated results of 25 September 2017.

Figure 3.5 illustrates the plot of fitted linear model describing the relationship between measured and simulated room temperature. Since the  $P$ -value is less than 0.05, there is a statistically significant relationship between measured room temperature and simulated room temperature at a 95.0 % confidence level. The  $R$ -Squared statistic indicates that the model as fitted explains 97.9296 % of the variability in measured room temperature. The correlation coefficient equals 0.989594, indicating a relatively strong relationship between the variables.

The standard error of the estimate shows the standard deviation of the residuals to be 0.484235. The mean absolute error of 0.383805 is the average value of the residuals.

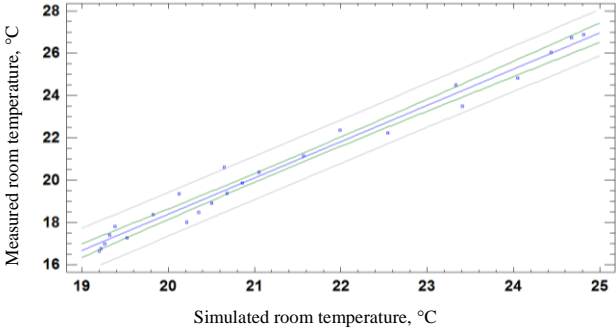


Fig. 3.5. Fitting of measured and simulated room temperatures.

Results of fitting a linear model to describe the relationship between measured PCM temperature and simulated PCM temperature are presented in Figure 3.6. The *P*-value is less than 0.05, thus there is a statistically significant relationship between the measured PCM temperature and simulated PCM temperature at a 95.0 % confidence level. The *R*-Squared statistic indicates that the model as fitted explains 93.3028 % of the variability in measured PCM temperature. The correlation coefficient equals 0.965934, indicating a relatively strong relationship between the variables. The standard error of the estimate shows the standard deviation of the residuals to be 1.12314. The mean absolute error of 0.810186 is the average value of the residuals.

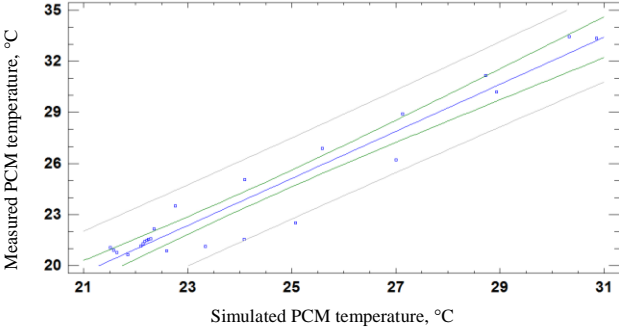


Fig. 3.6. Fitting of measured and simulated PCM temperatures.

The validation results confirm that the data resulting from the mathematical simulation is approximated in line with measurements carried out in real conditions. Consequently, the calculation model is valid for further research to compare the different design types and modelling under different climatic conditions.

### 3.5. Simulation results analysis

Two different alternatives were compared: solar facade module as described in Section 2.1.3 (A1), and opaque wall *U*-value 0.2 W/(m<sup>2</sup>K) (A2).

In the reference model, the solar facade module has been replaced by thermal insulation. The physics used are (Fig. 3.7): (a) heat transfer in solids for thermal insulation and (b) heat transfer in fluids for airspace. External plane (acrylic glass) is exposed to external conditions (including solar radiation) (c), other planes are bordering thermal insulation (d). The parameter

used for the output data of the reference wall model is indoor temperature. Each simulation setting uses the same initial values for both boxes, with the same starting temperature for all elements of both models.



Fig. 3.7. The boundary conditions for the model (marked blue).

Solar radiation is added to Module A2 on the external surface along with other external climate data. In Module A1, solar radiation for the core is indicated at a concentrated point analogue for real climate data.

Both alternatives were simulated for one sunny day in each of seasons and midseason: summer, winter, late autumn and early autumn. The early autumn day simulation is analogous to the late spring day, but the late autumn day is analogous to the early spring day, as average temperatures of outdoor air are similar and sun radiation differences are not substantial. No internal heating source is included in the simulation.

Simulated room and PCM temperatures, outdoor temperature and solar radiation for a summer day are presented in Figure 3.8. All temperatures are set to +19 °C at the beginning of the simulation, i.e. PCM is solid. Temperatures start to increase after the sunrise. However, the rate is different for both alternatives: the highest rate is for A1 followed by A2. Temperature of PCM in A1 increases with high rate and reaches +49 °C at its maximum.

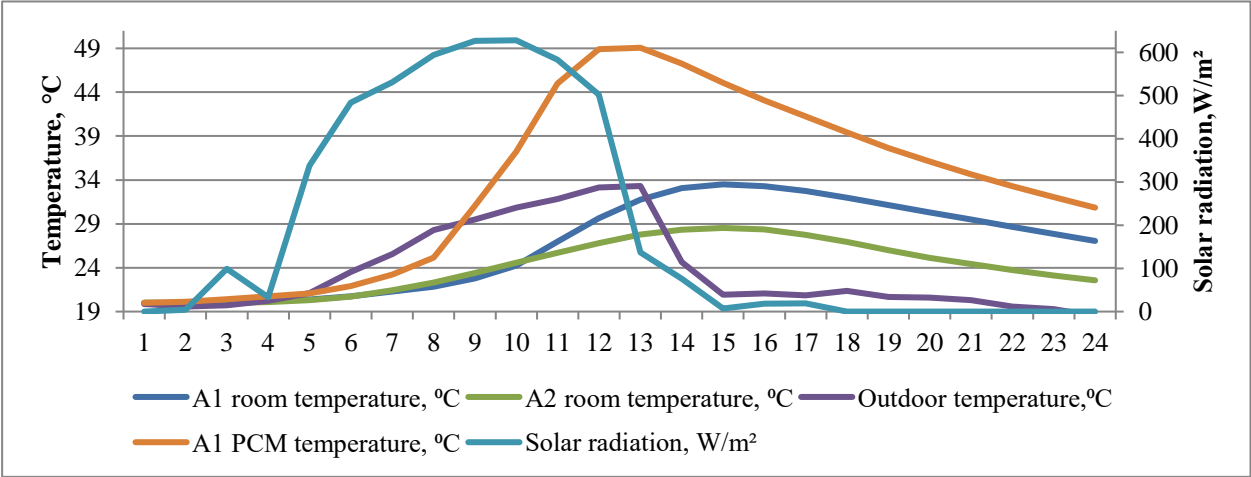


Fig. 3.8. Simulated room and PCM temperatures, outdoor temperature and solar radiation for a summer day.

Figure 3.9 presents temperature distribution and temperature difference in both alternatives in the 6th hour of the summer day. Lower temperature is observed at the bottom boundary because it is made from plywood and it works as thermal bridge.

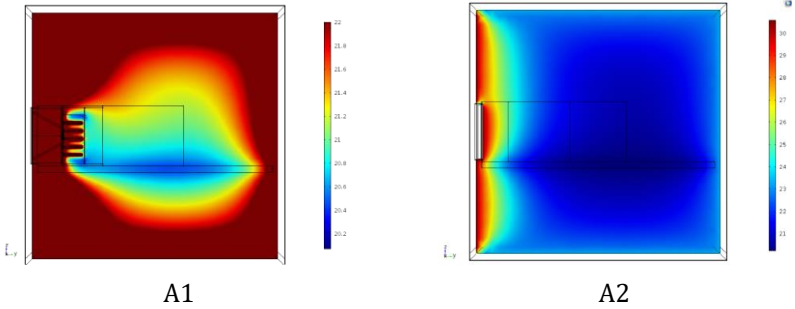


Fig. 3.9. Temperature distribution in the 6th hour of the summer day in both alternatives.

Figure 3.10 illustrates the dynamics of simulated room temperatures for both alternatives, PCM temperature for A1 as well as outdoor temperature and solar radiation for an early autumn day. The highest room temperature is reached if the solar facade module (A1) is used, followed by opaque wall (A2). The dynamic trend of both temperatures is similar, including the delay from the solar radiation. The PCM temperature rises in A1 and reaches +30.8 °C due to solar radiation. Compared to the summer day PCM temperature is ~ 18 °C lower. The main cause of such a difference is heat losses to outdoors generated by the temperature difference between the module and the outdoor temperature, which is greater than the solar influx into the module.

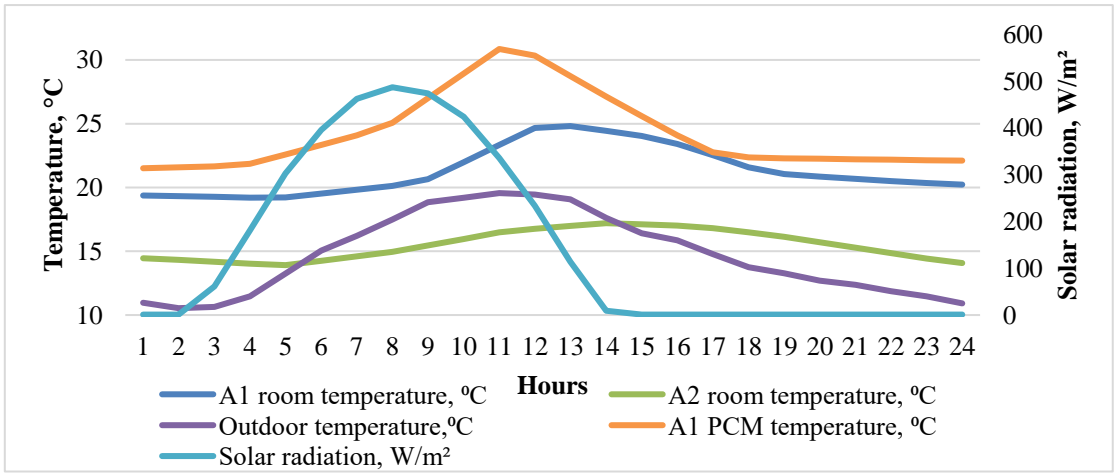


Fig. 3.10. Simulated room and PCM temperatures, outdoor temperature and solar radiation for an early autumn day.

Simulated room and PCM temperatures, outdoor temperature and solar radiation for a late autumn day are presented in Figure 3.11. The solar radiation is like in the early autumn day (Fig. 3.11), the outdoor temperature is much lower, which has an impact on the heat flow dynamics. At the beginning of the day all temperatures are set at 0 °C. Room temperature in both alternatives is increasing with similar trend. The highest temperature is reached in A1, followed by A2. Heat losses to the outdoors are higher compared to the early autumn day due to higher temperature difference between the PCM and the outdoor temperature.

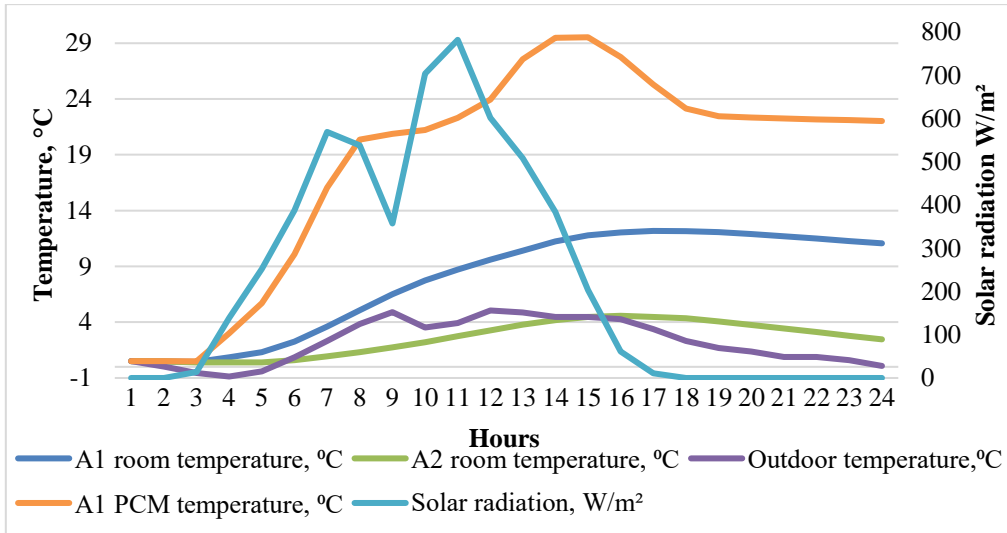


Fig. 3.11. Simulated room and PCM temperatures, outdoor temperature and solar radiation for a late autumn day.

During the winter, outdoor temperature falls below 0 °C and the solar energy is available with less intensity and for less hours per day (Fig. 3.12). Simulation starts at the outdoor temperature -12 °C. Solar energy collected by A1 can increase room temperature to max -9.5 °C, but for A2 to -11.5 °C. The room temperature is falling at a slower rate than the outdoor temperature.

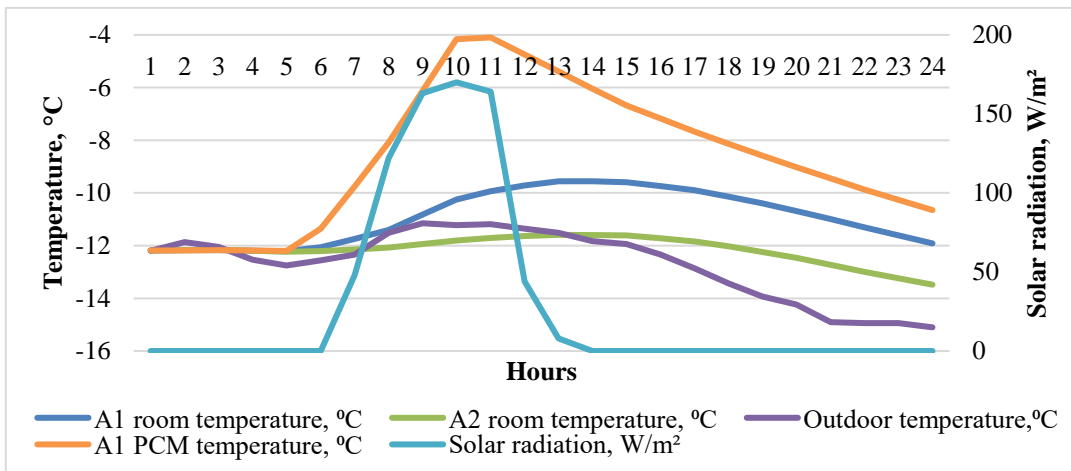


Fig. 3.12. Simulated room and PCM temperatures, outdoor temperature and solar radiation for a winter day.

The created solar facade module Bi-SES-II is suitable for deployment in the south-facing building envelope surfaces, both rooftops and facades. The module needs to lie in direct sunlight conditions. The shading of the surrounding environment will reduce the efficiency of the module and the possibility of storing solar power.

## 4. CLIMATE ADAPTIVE FACADE MODULE BI-SES INCORPORATED IN BUILDING

The building of the Latvian Museum of Contemporary Art (LMOCA) has been chosen as an example for the use of the solar facade module Bi-SES in new buildings. In the design of this building it is not possible to comply with all the design principles of the low energy buildings when faced with the functional limitations. The next chapters will explore the possibilities of integrating the developed solar facade module Bi-SES in the building envelope.

**Building location, function.** The design of the building of the Latvian Museum of Contemporary Art, after winning the architectural design contest, has been entrusted by the architect, Sir David Adjaye, Adjaye Associates. The museum building is in Riga in the newly developed block of New Hansa City. In the eastern and western directions, residential and administrative buildings up to 14 floors will be in adjacent blocks; the number of floors allowed for buildings on the south side is 7. On the north side, the building borders the park.

**General information.** The rectangular geometry of the plot has largely influenced the form of the building. The exterior shape of the building has a restrained form derived from the rectangle, with expressive triangular-shaped roof planes with varying roof slopes. The building has one underground floor and two above ground floors. The total height of the building above the ground at the highest point is 20 m. The underground floor is 3.5 m below the street level.

**Integrating Bi-SES to reduce LMOCA building energy demand.** There is not much glazing in the building's south facade. The LMOCA building longitudinal facades are oriented in south-north directions. In order to create optimal conditions for exposing artworks and to ensure their storage requirements, museum buildings have specific requirements for artificial and natural lighting. Location of transparent structures cannot be guided by maximising solar heat gains; it shall be governed by the lighting requirements. Each artwork may have specific lighting requirements from 100 % natural lighting to a completely darkened room. For natural lighting, the northern light is the most appropriate. Figure 4.1 reflects the lighting options of north-facing gallery.



Fig. 4.1. Example of lighting analysis of the LMOCA building gallery.

Contrary to the principles of the typical low-energy building design, the northern facade of the LMOCA building has extensive glazing, while the south facade of the building has only a small proportion of transparent surfaces. In Figure 4.2 and Figure 4.3, the glass planes are marked light blue. Thus, the developed Bi-SES modules can be placed in the south facade. Storing energy would reduce the energy consumption maintaining the microclimate in the building. Available area on the southern facade is 1097.4 m<sup>2</sup>.

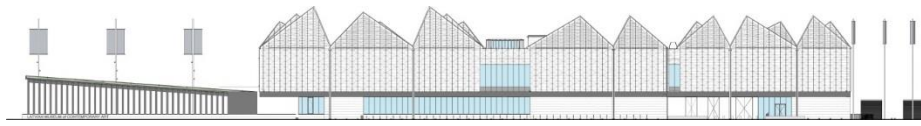


Fig. 4.2. South facade.



Fig. 4.3. North facade.

On the first floor there will be cast in situ three-layer concrete walls, while the second-floor facade and roof planes are designed as ventilated structures with vertical posts. On the second floor and on the roof planes, dolomite cladding will be used. Following the architect's intention to separate the building floors, the elements of Bi-SES are proposed to be placed in the planes of the second floor and roof.

**Shading studies of LMoCA building.** The Bi-SES element is designed as a solar energy capturer, so it is effective to place it in the planes that receive the most solar radiation.

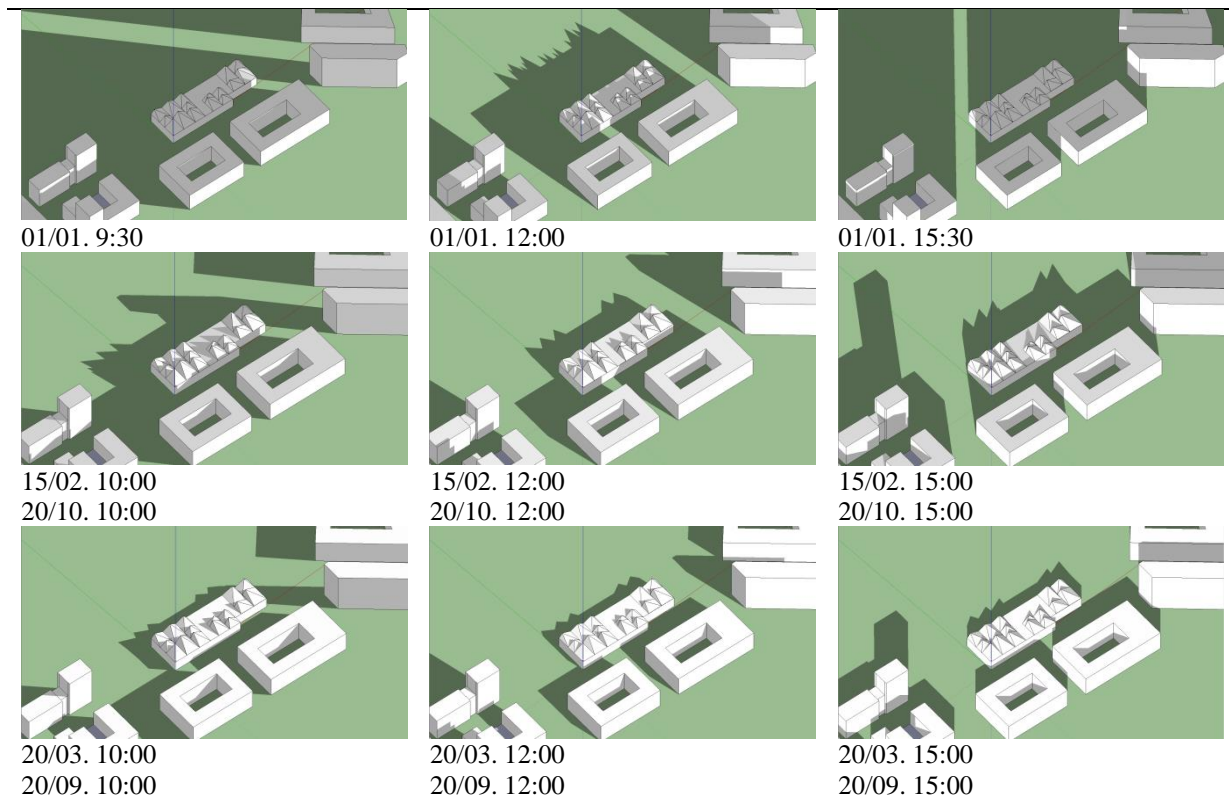


Fig. 4.4. Shading Studies.

Figure 4.4 shows the shading studies of the LMoCA building in the surrounding environment (Sketchup). In January, at the lowest angle of sun, the building is nearly 100 % shaded throughout the day. From February 15 to October 20, the 1st row of rooftop planes will

be unshaded throughout the day. The south facade will be unshaded between March 20 and September 22. Roof planes behind the first row are shaded by other roof planes in front, so the deployment of Bi-SES in these planes is not considered.

The building’s shading studies show that the building’s south facade is unshaded between April and early September. But the south-facing rooftop planes in the first row are unshaded for a longer period, from mid-February to early October.

***Incorporation of Bi-SES element into LMoCA building envelope to reduce energy consumption for heating and cooling of the building.*** Three Bi-SES deployment scenarios are explored (Fig. 4.5): Scenario I – in the 2nd floor walls of southern facade (green); Scenario II – in south-oriented roof planes (red); Scenario III – combination of Scenario I and II, Bi-SES are located in both the facade and roof planes (green + red). The number of Bi-SES elements and the total volume of PCM according to the scenarios is described in Table 4.14.1.

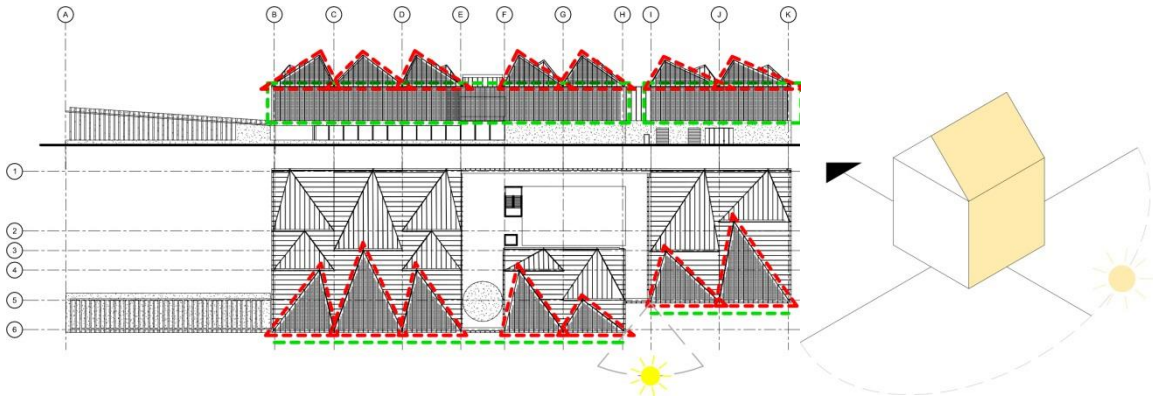


Fig. 4.5. Bi-SES location in Scenario I – in S facade walls (green) and in Scenario II – in roof planes (red).

Table 4.1

Total Number of Bi-SES According to Scenarios

No.	Description	Number of elements	PCM volume, m <sup>3</sup>
I	2nd floor wall	10 400	5.98
II	Roof planes	7200	4.14
III	2nd floor wall + roof planes	17 600	10.12

The minimum number of elements to be deployed is 7200 elements (Scenario II) or ~ 4 m<sup>3</sup> of phase change material, but if Bi-SES is placed on both the facade and roof planes, the total volume of PCM reaches 10 m<sup>3</sup>.

## CONCLUSIONS

1. To achieve higher building energy efficiency targets, innovative building thermal envelope design concepts are needed. Building thermal envelope has to become an active part of building energy balance gaining dynamic properties.
2. The main goal of this research is to study the storage capacity and dynamic behaviour of developed solar facade module that can accumulate energy to reduce heating and cooling loads in nearly zero energy building. The module comprises a combination of PCM, granulated aerogel, Fresnel lens and copper heat transfer enhancers.
3. The aim of the research is to develop an innovative biomimicry based thermal envelope design. Comparing thermoregulatory strategies with the multi-criteria method, as the most suitable example for imitation in building envelope was chosen blubber – the subcutaneous fat layer found in arctic mammals.
4. Following the biomimicry approach, imitating the thermoregulation processes in the subcutaneous fat layer and adding a light-focusing concept found in brittle star surface, an innovative solar facade module was developed. It captures and accumulates solar energy during the day and transfers it to the room at night, reducing heating and cooling loads in nearly zero-energy buildings. The storage capacity and dynamic behaviour of this facade module was studied. The developed module consists of phase change material, aerogel, Fresnel lens and copper heat transfer enhancers.
5. The study shows that the dynamics of heat flows and accumulation processes in the developed solar facade module are very complex due to highly changing outdoor and indoor conditions. Experimental results show that the dynamic behaviour of the room temperature and heat flux in the reference box made from mineral wool differs from the same parameters measured in the solar facade module. Heat flux in the reference box coincides with the delayed solar radiation and at its maximum peak is around four times less than in the solar facademodule. The room temperature in the reference box differs from the module between 0.5 °C during the day and 5 °C during the night due to the impact of the thermal energy accumulation in the PCM. The time lag between the solar radiation and PCM temperature is 3.5 h, while between the PCM temperature and indoor temperature it is 45 min. Indoor temperature peak in the reference box is delayed from the solar radiation peak by 4 h.
6. Simulation results show that when two different alternatives are compared (the solar facade module (A1), and the opaque wall (A2)), in four sunny days representing summer, winter, late autumn and early autumn, higher room temperature can be reached with the solar facade module. The indoor temperature difference in the range of 0.5 °C and 9 °C is observed between the opaque reference wall and the solar facade module depending on the time of the day and season. The dynamics of room temperatures in both alternatives are influenced by the solar influx into the module, and the temperature difference between the PCM and the outdoor temperature in the case of A1, and the room and outdoor temperature in the case of A2. Simulation also shows that the change of PCM volume can either increase or decrease the accumulated latent energy.

7. To sum up, the study findings demonstrate that the use of the Fresnel lens for solar radiation concentration combined with insulation material with low thermal conductivity can increase indoor temperature and reduce building energy consumption for heating compared to opaque wall. The findings agree with the results from other studies, e.g. studies on solar wall integrating phase change material [25], thermal behaviour of a passive solar wall with silica aerogel and phase change materials [26], application of PCM in buildings in a mild climate [27], and numerical simulation of lightweight concrete wall combined with aerogel and PCM [26].
8. Future studies will include moving layer of translucent silica aerogel granules, which is used to reduce thermal losses from the element when solar energy is absent, as well as solar tracking system and automation control. Further studies will also assess the impact of reduction of copper plate size or even replacement with more compact shape of heat transfer enhancers to reduce heat losses from the PCM to outdoors. Assessment of seasonal accumulation of energy within the module will be carried out.

## REFERENCES

- [1] J. M. Benyus, *Biomimicry: Innovation Inspired by Nature*, HarperCollins Publishers Inc., 1997.
- [2] S. Gosztonyi, M. Brychta, P. Gruber, “Challenging the engineering view: comparative analysis of technological and biological functions targeting energy efficient facade systems,” %1 *Design and Nature V*, Pisa, Italy, 2010.
- [3] Neil A. Campbell, Jane B. Reece, Lawrence G. Mitchell, *Biology*, 5th edition, Benjamin/Cummings, 1999.
- [4] K. Schmidt-Nielsen, *Animal Physiology: Adaptation and Environment*, Cambridge University Press, 1997.
- [5] Richard W. Hill, Gordon A. Wyse, Margaret Anderson, *Animal Physiology*, Sinauer Associates, Inc, 2012.
- [6] E. S. E. Hafez (editor), W. Bianka, “Adaptation of Domestic Animals,” %1 *Termoregulation*, Philadelphia, Lea & Febiger, 1968, pp. 97–118.
- [7] D. M. Gates, *Biophysical Ecology*, New York: Springer – Verlag, 1980.
- [8] C. A. DiMarzio, *Optics for Engineers*, Boca Raton: CRC Press; Taylor & Francis Group, LLC, 2012.
- [9] Annalisa Berta, James L. Sumich, Kit M. Kovacs, *Marine Mammals: Evolutionary Biology*, London: Academic Press, Elsevier, Inc., 2005.
- [10] Struntz D. J., McLellan W. A., Dillaman R. M., Blum J. E., Kucklick J. R., Pabst D. A., “Blubber development in bottlenose dolphins (*Tursiops truncatus*),” *Journal of Morphology*, sēj. 259, nr. 1, pp. 7–20, 2004.
- [11] Bernd Würsig, William Perrin, Bernd Würsig, J.G.M. Thewissen, *Encyclopedia of Marine Mammals*, 2nd Edition, London: Academic Press, Elsevier, Inc, 2008.
- [12] Paul Ehrlich, David S. Dobkin, Darryl Wheye, *Birder’s Handbook: A Field Guide to the Natural History of North American Birds*, New York: Touchstone, Simon & Schuster, Inc., 1988.
- [13] E. M. a. M. Pereyra-Rojas, “Understanding the Analytic Hierarchy,” %1 *Practical Decision Making*, SpringerBriefs, 2017, pp. 7–17.
- [14] M. Majumder, *Impact of Urbanization on Water Shortage in Face of Climatic Aberrations*, Springer, 2015.
- [15] <https://asknature.org/> [Online]. [Accessed 1.12.2018.].
- [16] Pat Willmer, Graham Stone, Ian Johnston, *Environmental physiology of animals*, Blackwell Science, Ltd., 2005.
- [17] Sari A., “Eutectic mixtures of some fatty acids for low temperature solar heating applications: Thermal properties and thermal reliability,” *Applied Thermal Engineering*, vol. 25, pp. 2100–2107, 2005.

- [18] Sari A., Karaipekli A., "Preparation and thermal properties of capric acid/palmitic acid eutectic mixture as a phase change energy storage material," *Materials Letters*, vol. 62, pp. 903–906, 2008.
- [19] Yuan Y. et al., "Fatty acids as phase change materials: A review," *Renewable and Sustainable Energy Reviews*, no. 29, pp. 482–498, 2014.
- [20] Karaipekli A., Sari A., "Preparation, thermal properties and thermal reliability of eutectic mixtures of fatty acids/expanded vermiculite as novel form-stable composites for energy storage," *Journal of Industrial and Engineering Chemistry*, vol. 16, pp. 767–773, 2010.
- [21] "Rubitherm," 28.03.2015. [Online]. Available: <http://www.rubitherm.com/english/index.htm>
- [22] 10.11.2017. [Online]. Available: <https://www.edmundoptics.com/optics/optical-lenses/fresnel-lenses/5.0quot-x-5.0quot-2.8quot-focal-length-fresnel-lens/#downloads>
- [23] "Rubitherm Technologies GmbH," 10.11.2017. [Online]. Available: [https://www.rubitherm.eu/media/products/datasheets/Techdata\\_-RT21HC\\_EN\\_29062016.PDF](https://www.rubitherm.eu/media/products/datasheets/Techdata_-RT21HC_EN_29062016.PDF)
- [24] "www.Comsol.com," Comsol, 21.05.2018. [Online]. Available: <https://www.comsol.com/heat-transfer-module> [Accessed 5.21.2018.].
- [25] Karunesh Kant, A. Shukla, Atul Sharma, "Advancement in phase change materials for thermal energy storage applications," *Solar Energy Materials and Solar Cells*, vol. 172, pp. 82–92, 2017.
- [26] Mohammad H. Baghban, Per J. Hovde, Arild Gustavsen, "Numerical Simulation of a Building Envelope with High Performance Materials," Paris, 2010.
- [27] Michal Pomianowski, Per Heiselberg, Yinping Zhang, "Review of thermal energy storage technologies based on PCM application in buildings," *Energy and Buildings*, vol. 67, pp. 56–69, 2013.